Bioorganic & Medicinal Chemistry 21 (2013) 4158–4169

Contents lists available at SciVerse ScienceDirect

Bioorganic & Medicinal Chemistry

journal homepage: www.elsevier.com/locate/bmc

Synthesis and bioactive evaluation of novel hybrids of metronidazole and berberine as new type of antimicrobial agents and their transportation behavior by human serum albumin

Ling Zhang, Juan-Juan Chang, Shao-Lin Zhang, Guri L. V. Damu †, Rong-Xia Geng *, Cheng-He Zhou *

Laboratory of Bioorganic & Medicinal Chemistry, School of Chemistry and Chemical Engineering, Southwest University, Chongqing 400715, PR China

ARTICLE INFO

Article history:
Received 30 March 2013
Revised 6 May 2013
Accepted 7 May 2013
Available online 16 May 2013

Keywords:
Imidazole
Metronidazole
Berberine
Antibacterial
Antifungal
Human serum albumin

ABSTRACT

A series of novel hybrids of metronidazole and berberine as new type of antimicrobial agents were synthesized and characterized by ^{1}H NMR, ^{13}C NMR, IR, MS and HRMS spectra. Bioactive assay manifested that most of the prepared compounds exhibited effective antibacterial and antifungal activities and some showed comparable or superior potency against *Methicillin-resistant Staphylococcus aureus* to reference drugs Norfloxacin, Chloromycin and Berberine. The transportation behavior of human serum albumin (HSA) to the highly active compound **5g** was evaluated and revealed that the association of imidazole derivative **5g** with HSA was spontaneous and the electrostatic interactions played important roles in the transportation of HSA to **5g**. The calculated parameters indicated that compound **5g** could be effectively stored and carried by HSA.

1. Introduction

Imidazole derivatives have been attracting increasing interest due to their large potentiality in medicinal chemistry.[1–6] Nitro modified imidazoles are a unique type of imidazole derivatives in which nitro fragment could not only enhance lipophilicity of the target compounds which is favorable for tissue penetration, but also induce bioactivities through the metabolic activation of nitro group.[7] Nitroimidazole-based compounds exhibited various bioactivities like antibacterial,[8,9] anti-tubercular,[10] antiparasitic[11] and anticancer[12,13] ones. Especially, as antimicrobial agents, many nitroimidazoles such as metronidazole, benznidazole, ornidazole, secnidazole, nimorazole and tinidazole have been in widespread clinical use to treat diseases caused by anaerobic bacteria.[4,14] Notably, despite of their long term clinical use, the incidence of resistance in anaerobic bacteria is still very low. This encourages continuous researches to focus on the development of such nitroimidazoles with potential medicinal application. Particularly, structurally simple metronidazole as an effective synthetic drug introduced in 1960 possesses strong inhibitory efficacies against Gram-negative anaerobic bacteria like *Helicobacter pylori* and protozoa such as *Giardia*, *Lamblia*, and *Entomoeba histolytic*.[15] However, with the extensive investigations towards nitroimidazoles, researches disclosed that the reactive intermediates formed in microorganisms by the reduction of nitro group in nitroimidazoles could covalently bind with DNA and trigger the adverse effect. The sterical protection of nitro group in metronidazole was proved to be an effective way to improve the metabolism and physicochemical property of such compounds.[16] Furthermore, some frequently used clinical antimicrobial nitroimidazole drugs like nitroimidazooxazine PA-824 were reported to be subjected to poor aqueous solubility and unsuitable binding propensity to proteins in human plasma (Fig. 1).[17–19] Therefore, the development of new types of nitroimidazoles with broad antimicrobial spectrum, good metabolism and physicochemical property, and suitable binding affinity to serum albumins has been recently attracting special attention. Much effort has been oriented towards novel nitroimidazole-based antimicrobial agents with high efficiency.

Berberine has been commonly used in the clinic as therapeutic agent to treat infectious diseases such as acute gastroenteritis, cholera and bacillary dysentery for many years. Its importantly clinical uses stimulate the continuing researches in antimicrobial field[20,21] and other related investigations such as anticancer,[22] antiviral,[23] antiinflammatory,[24] antiparasitic[25,26] activities. The special structure of berberine with a quaternary nitrogen and large desirable π-conjugated backbone could exert noncovalent forces like π–π stacking and electronic interactions. Thereby, it not only could improve the physicochemical properties of its derivatives,

* Corresponding authors. Tel./fax: +86 23 68254967.
E-mail addresses: geng0712@swu.edu.cn (R.-X. Geng), zhouch@swu.edu.cn (C.-H. Zhou).
† Postdoctoral fellow from Indian Institute of Chemical Technology (IICT), Hyderabad 500 607, India.

0968-0896/$ - see front matter © 2013 Elsevier Ltd. All rights reserved.
http://dx.doi.org/10.1016/j.bmc.2013.05.007

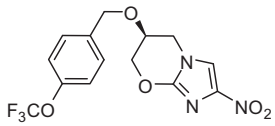

Nitroimidazooxazine (PA-824)

Figure 1. Structure of nitroimidazooxazine (PA-824).

their affinity to transport proteins, and thus enhance their antimicrobial activities, but also easily interact with diverse enzymes and receptors in biological system resulting in broad bioactive spectrum. In our previous work,[27] a type of amine-derived bis-azoles has been successfully developed as newly structural Fluconazole analogues. The tertiary alcohol moiety in Fluconazole was replaced by a tertiary amino group as bioisoster, and the methylene bridge between the tertiary alcohol and the triazolyl moieties was substituted by an ethylene chain (Fig. 2). Bioactive study manifested that this type of compounds exhibited good or even better antimicrobial activities in comparison to reference drugs Chloromycin, Norfloxacin and Fluconazole. Here, we would like to replace the azolyl ethylamino moiety with the clinical metronidazole as bioisoster fragment and further substitute the other azolyl ring by the berberine skeleton to generate a series of novel hybrids of berberine and nitroimidazoles as potential antimicrobial agents. This special type of hybrids might not only be helpful to spatially protect the nitro group with the potential to improve the metabolism and physicochemical property, but also improve the water solubility and binding affinity by the introduction of tertiary amine moiety thereby effectively increase their biological activities and broaden active spectrum. In addition, various halobenzyl moieties were introduced into target compounds to investigate the effect of halobenzyl moiety on biological activities, since many halobenzyl incorporated molecules gave good antimicrobial activities.[28,29] The designed structures of this series of novel hybrids of berberine and nitroimidazole moiety including 4-nitroimidazole, 5-nitroimidazole and 2-methyl-5-nitroimidazole derivatives are shown in Scheme 1.

Serum albumins as the most important and abundant macromolecule proteins in the circulatory system have received much attention for that they could deliver drugs or other bioactive small molecules to the binding sites.[30,31] A thorough binding analysis between drugs or bioactive small molecules and human serum albumin (HSA) may beneficially provide useful information for the absorption, transportation, distribution, metabolism and excretion properties of drugs. It might also be significant to the design, modification and screening of drug molecules. In view of above observations, it is considerably reasonable for us to further investigate the transportation behavior by HSA to the highly active prepared compounds in order to preliminarily evaluate their transportation and pharmacokinetic properties by fluorescence and UV–vis absorption spectroscopy on molecular level.

2. Results and discussion

2.1. Chemistry

The target hybrids of berberine nitroimidazoles were prepared from commercial halobenzyl chlorides, diethanolamine and berberrubine (Scheme 1). Diethanolamine was *N*-alkylated with different halobenzyl chlorides **1a–e** to produce intermediates **2a–e** in excellent yields (92.2–97.8%). The resulting diols **2a–e** were treated in chloroform with phosphorus tribromide to afford dibromides **3a–e** in good yields ranging from 88.3% to 97.4%.[27] Further reactions of compounds **3a–e** with 4-nitroimidazole afforded the corresponding mono-azole bromides **4b–k** in 18.5–80.2% yields. Possible reactions of 4-nitroimidazole in the presence of potassium carbonate are shown in Figure 3. It has been documented that tautomeric interconversion of the 5-nitro and 4-nitro imidazoles takes place under either acidic or basic conditions. During the *N*-alkylations of 4-nitroimidazole with alkyl halides, the acidic conditions favored the 5-nitro orientation while basic conditions favored the 4-nitro orientation.[32] In this work, potassium carbonate was selected to produce our target compounds, since the yields were generally poor under acidic conditions. In the presence of potassium carbonate, 4-nitroimidazole displays four resonance forms (**A–D**) (Fig. 3). Since patterns **A** and **C** are much more stable than patterns **B** and **D**, the *N*-alkylation of 4-nitroimidazole could yield *N*-1 and *N*-3 alkylated products, and the former is the predominant one due

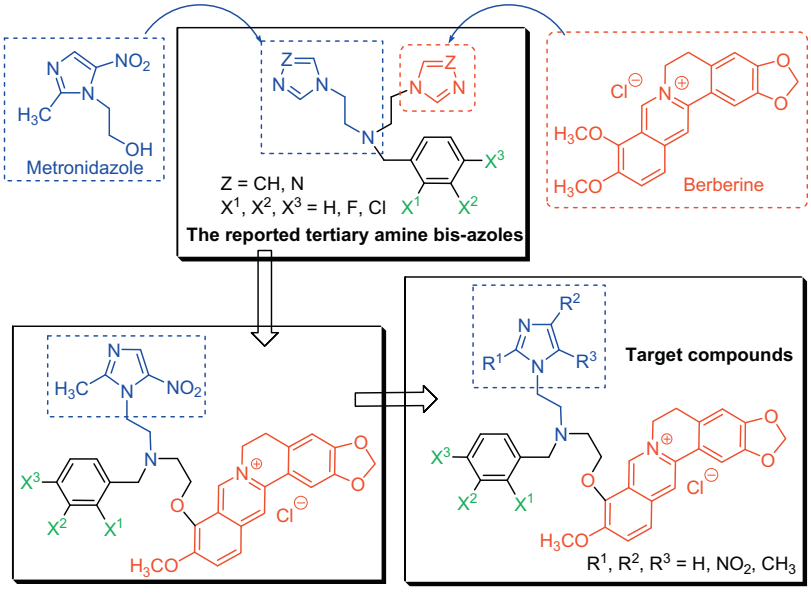

Figure 2. Design of novel hybrids of berberine and nitroimidazoles.

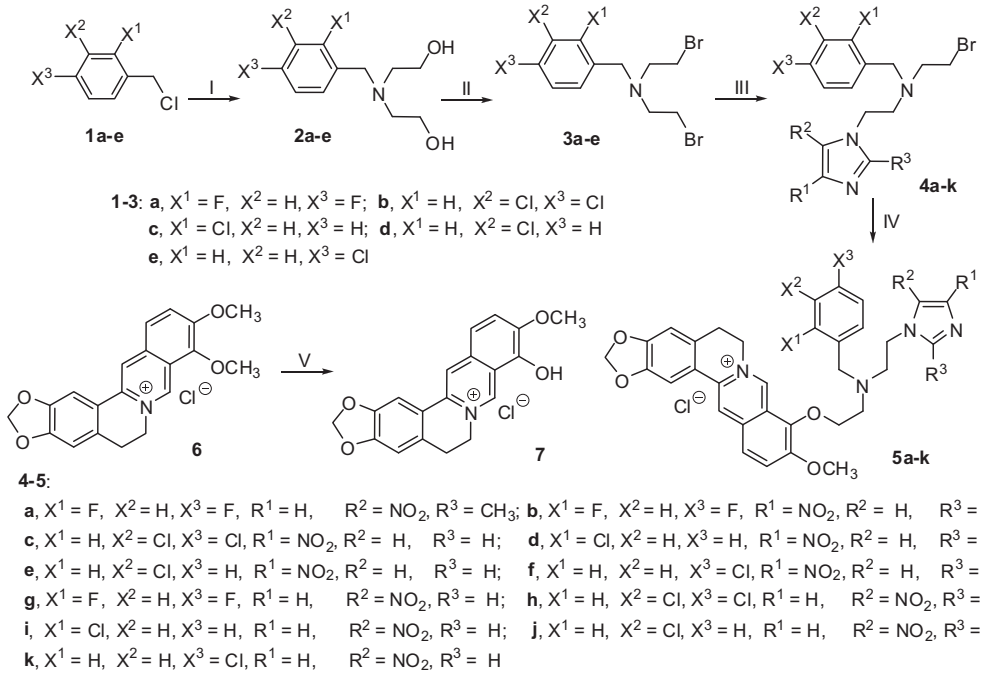

Scheme 1. Synthetic route of berberine nitroimidazoles. Reagents and conditions: (I) CH_3CN, diethanolamine, 50 °C, 10–12 h, yields 92.3–98.6%; (II) $CHCl_3$, PBr_3, refluxed, 2 h, yields 88.1–98.5%; (III) 4-nitroimidazole or 2-methyl-5-nitroimidazole, K_2CO_3, CH_3CN, 60 °C, 10–12 h, yields 18.4–80.2%; (IV) berberrubine, DMF, 110 °C, 20 h, yields 23.0–38.7%; (V) berberine, 20 mm Hg, 190 °C, 15 min, yield 88.4%.

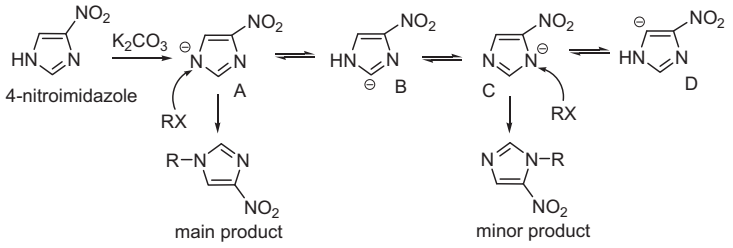

Figure 3. Possible reactions of 4-nitroimidazole in the presence of potassium carbonate.

to the relative low acidity of –NH– proton compared to 5-nitroimidazole. Actually, synthesis of 5-nitroimidazole derivatives has rarely been reported,[33,34] which is probably due to the nonavailability of 5-nitroimidazole. In the preparations of 4-nitroimidazoles **4b**–**f**, 5-nitroimidazole derivatives **4g**–**k** were obtained as by-products. As for 2-methyl-5-nitroimidazole, the presence of the methyl substituent at *C*-2 possibly reduces the acidity of the –NH– protons induced by the nitro group at the *C*-5 position. Therefore, the reaction of compound **3a** with 2-methyl-5-nitroimidazole afforded a single product **4a**.

Generally, there are two kinds of reported methods for demethylation of berberine chloride including fusion with pyridine hydrochloride and thermal decomposition. The first method was lack of selectivity, while the second one could selectively and conveniently produce demethylation at 9-position. Possibly, under the reduced pressure (20 mm Hg) at 190 °C, berberine could generate the ketoform intermediate, which could be easily converted into berberrubine in the presence of hydrochloric acid.[35–37] In this work, berberrubine **7** was prepared in 88.4% yield by demethylation of berberine chloride **6** at 190 °C under reduced pressure (20 mm Hg) for 15 min.

Finally, target nitroimidazoles **5a**–**k** were conveniently obtained by the alkylation of berberrubine **7** with a series of corresponding compounds **4a**–**k** in DMF at 110 °C for 20 h in practical yields (23.0–38.7%).

2.2. Spectral analysis

All newly synthesized compounds were characterized by ^1H NMR, ^{13}C NMR, IR, MS and HRMS spectra. The spectral analyses were in accordance with the assigned structures, and listed in the experimental section.

2.2.1. IR spectra

In IR spectra, compounds **4a**–**k** gave moderate absorption bands at 3085–3014 cm^{-1} and 2971–2821 cm^{-1} attributed to the stretching vibration of aromatic and aliphatic C–H, respectively. While the aromatic frame exhibited characteristic stretching frequencies in the region between 1603 and 1482 cm^{-1}. All target compounds **5a**–**k** gave moderate absorption at 3152–3011 cm^{-1} due to the stretching vibration of aromatic C–H. The absorption bands ascribed to aliphatic C–H stretching vibrations were seen at two regions of 2972–2921 and 2857–2816 cm^{-1}, while the aromatic frame exhibited characteristic stretching frequencies in the region of 1601–1474 cm^{-1}. Furthermore, two strong and sharp peaks at 1570–1528 and 1350–1341 cm^{-1} in compounds **5a**–**k** were

attributed to the vibration of N=O bond. All the other absorption bands were also observed at expected regions.

2.2.2. ^{1}H NMR spectra

In ^{1}H NMR spectra, for compounds **4b**–**k**, it is expected that chemical shift values of H^c proton in 5-nitroimidazole derivatives **4g**–**k** (Table 1) should be more downfield, due to the adjacence of strong electron-withdrawing nitro group, than the 4-nitroimidazoles **4b**–**f**. In this case, protons at 4.39–4.31 ppm were attributed to the H^c protons of 5-nitroimidazoles **4g**–**k**, while compounds with similar peak at 4.06–3.98 ppm were identified as the 4-nitroimidazole isomers **4b**–**f**. Additional evidence supporting the present structural assignment can be obtained from the chemical shift values of H^a and H^d protons. The H^d protons between the nitro group and a sp^2 nitrogen in 5-nitro isomers **4g**–**k** (7.92–7.84 ppm) were expected to be more downfield than the H^a protons (7.75–7.67 ppm) placed between the nitro group and a sp^3 nitrogen in the 4-nitro isomers **4b**–**f**. In the ^{1}H NMR spectra of compounds **5b**–**k**, 4-nitroimidazoles **5b**–**f** (8.19–7.83 ppm) gave higher shifts for H^a when compared with precursors **4b**–**f** (7.75–7.67 ppm), while 5-nitroimidazoles **5g**–**k** (7.89–7.79 ppm) displayed relatively lower shifts for H^d than corresponding **4g**–**k** (7.92–7.84 ppm).

2.2.3. ^{13}C NMR spectra

The ^{13}C NMR spectral analyses were in accordance with the assigned structures. No large differences were found in ^{13}C chemical shifts after the conversions of compounds **4a**–**k** into nitroimidazoles **5a**–**k**. The signals at 162.7–157.9 and 163.8–150.5 ppm in compounds **4a–k** and **5a**–**k** were assigned to the halo attached carbons. The carbons connected with nitro group in compounds **4** and **5** gave relative high signals at δ 139.1–135.5 ppm and the ^{13}C chemical shifts of other carbons in nitroimidazole ring were observed at δ 136.0–131.0 ppm, while all the other carbons gave ^{13}C peaks at the expected regions.

2.3. Biological activity

All newly synthesized compounds **4a**–**k** and **5a**–**k** and their precursors were evaluated for in vitro antibacterial and antifungal activities against four Gram-positive bacteria (*Staphylococcus aureus* ATCC25923, *Methicillin-resistant S. aureus* N315, *Bacillus subtilis* ATCC6633 and *Micrococcus luteus* ATCC4698), four Gram-negative bacteria (*Escherichia coli* DH52, *Proteus vulgaris* ATCC6896, *Pseudomonas aeruginosa* and *Shigella dysenteriae*) and two fungal strains (*Candida albicans* ATCC76615 and *Candida mycoderma*) using two-fold broth dilution method in 96-well microtest plates recommended by National Committee for Clinical Laboratory Standards (NCCLS).[38] The biological tests were carried out in triplicate. Minimal inhibitory concentration (MIC, μg/mL) was defined as the lowest concentration of new compounds that completely inhibited the growth of bacteria. Currently available antimicrobial drugs such as Berberine, Chloromycin, Norfloxacin and Fluconazole were used as standard drugs.

Table 1
Some ^{1}H NMR data (δ ppm) of 4-nitroimidazole and 5-nitroimidazole derivatives **4b**–**k**

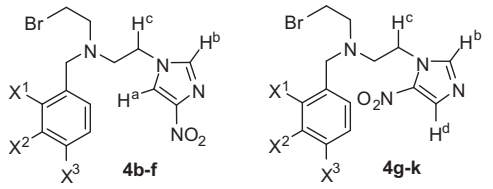

	4b	4c	4d	4e	4f	4g	4h	4i	4j	4k
H^a	7.71	7.75	7.73	7.69	7.67	––	––	––	––	––
H^b	7.48	7.47	7.52	7.43	7.45	7.69	7.67	7.66	7.65	7.66
H^c	4.06	4.03	3.99	3.98	3.99	4.36	4.33	4.39	4.31	4.32
H^d	––	––	––	––	––	7.86	7.91	7.84	7.90	7.92

2.3.1. Antimicrobial activity

The antimicrobial results as shown in Table 2 revealed that most of the prepared compounds **4** and **5** could effectively inhibit the growth of all tested strains in vitro. For the prepared nitroimidazoles **4a**–**k**, the tested strains were quite sensitive to compounds **4g** and **4i** with MIC values of 1–32 μg/mL. Especially, 2,4-difluorobenzyl derivative **4g** gave low inhibitory concentration (MIC = 8 μg/mL) towards *P. aeruginosa*, which was two times more active than clinical drug Clinafloxacin (MIC = 16 μg/mL). The anti-*C. mycoderma* activity (MIC = 4 μg/mL) also was comparable to reference drug Fluconazole (MIC = 4 μg/mL).

In comparison to their precursors **4a**–**k**, compounds **5a**–**k** displayed stronger antimicrobial efficacy and broader antimicrobial spectrum. Notably, some synthesized nitroimidazoles showed superior potency against MRSA to reference drugs Norfloxacin, Chloromycin and Berberine. Especially, 2,4-difluorobenzyl derivative **5g** and 2-chlorophenyl compound **5i** exhibited noticeable and broad spectrum antimicrobial activities against all the tested bacteria and fungi with MIC values of 1–32 μg/mL. Excitedly, bacteria MRSA was sensitive to the target compounds **5g** and **5i** with MIC values of 16 and 8 μg/mL, respectively, which were comparable to reference drugs Chloromycin (MIC = 16 μg/mL) and Norfloxacin (MIC = 8 μg/mL). Particularly, compound **5g** gave low inhibitory concentration towards *S. dysenteriae* and *P. vulgaris* with MIC values of 4 μg/mL, which were comparable to or even better than the reference drugs Chloromycin, Berberine and Norfloxacin. The anti-*C. mycoderma* activity (MIC = 1 μg/mL) also was fourfold more potent than the reference drug Fluconazole (MIC = 4 μg/mL). In addition, compound **5i** also exhibited good activity against *S. aureus* with MIC value of 2 μg/mL, which was eightfold and 256-fold more potent than Chloromycin and Berberine, respectively. It could also remarkably inhibit the growth of *B. subtilis* and *E. coli* with MIC values of 4 μg/mL, which were fourfold more potent than Chloromycin. These antimicrobial results manifested that the incorporation of berberine moiety into target compounds should be beneficial for the antibacterial and antifungal potency. To our surprise, generally all 4-nitroimidazoles **5b**–**f** displayed lower antimicrobial activities than that of 5-nitroimidazoles **5g**–**k**.

In view of above discussion, the antimicrobial efficacies should be closely related to nitroimidazole ring and halobenzyl group to some extent. For this serial compounds, nitroimidazoly moieties contributed to the antibacterial activities in the order of 5-niotroimidazoly >4-nitroimidazoly. Difluorobenzyl group was more helpful for increasing antibacterial and antifungal efficacy in comparison to other halobenzyl ones.[39]

2.3.2. Analysis of Log*P* values

Lipophilicity/hydrophilicity governs various biological processes such as the transportation, distribution, metabolism and secretion of biological molecules. A good knowledge of the lipophilicity/hydrophilicity is essential to predict the transportation and activity of drugs. Therefore, the lipophilicity/hydrophilicity expressed as octanol/water partition coefficient (Log*P*) was determined experimentally by traditional saturation shake flask method combining with UV–vis spectrophotometric approach (Supplementary data). According to the Lipinski's rule-of-five, all the synthesized compounds **5a**–**k** had desirable Log*P* values (no more than five) as given in Table 3. They had suitable lipophilicity that was favorable for them to permeate through biological membrane and to be delivered to the binding sites.

Table 2
In vitro antimicrobial activities for compounds **4**–**5** expressed as MIC (μg/mL)

Compds	Gram-positive bacteria				Gram-negative bacteria				Fungi	
	MRSA	*S. aureus*	*B. subtilis*	*M. luteus*	*E. coli*	*S. dysenteriae*	*P. aeruginosa*	*P. vulgaris*	*C. albicans*	*C. mycoderma*
4a	16	64	256	128	32	32	64	128	128	128
4b	64	32	64	16	32	16	16	32	32	8
4c	64	32	32	64	32	16	32	64	32	64
4d	64	16	32	64	32	32	32	64	16	128
4e	128	64	64	64	128	256	64	512	128	128
4f	128	64	64	128	128	128	256	128	64	128
4g	32	32	64	16	32	8	8	16	16	4
4h	32	32	32	128	16	8	16	32	16	128
4i	16	8	8	64	8	16	16	16	8	32
4j	64	16	64	64	64	256	32	256	64	64
4k	128	64	64	128	128	256	64	256	64	128
5a	16	16	64	128	128	256	128	64	64	128
5b	32	16	32	16	16	4	16	16	16	8
5c	64	16	32	16	16	4	16	16	16	64
5d	16	4	4	16	16	16	16	64	8	128
5e	32	8	32	64	32	256	64	64	16	32
5f	64	32	64	32	64	128	64	64	64	16
5g	16	8	32	8	8	4	8	4	8	1
5h	16	8	16	32	8	2	8	16	8	64
5i	8	2	4	32	4	8	8	16	4	32
5j	16	4	32	32	32	256	16	64	32	32
5k	32	16	128	64	32	32	16	32	32	64
A	16	16	32	8	32	32	32	32	—	—
B	8	0.5	1	2	16	4	16	8	—	—
C	128	512	>512	>512	>512	256	256	128	>512	128
D	—	—	—	—	—	—	—	—	1	4

[a]Minimum inhibitory concentrations were determined by micro broth dilution method for microdilution plates.
[b]**A** = Chloromycin, **B** = Norfloxacin, **C** = Berberine, **D** = Fluconazole.
[c]MRSA, *Methicillin-Resistant Staphylococcus aureus* N315; *S. aureus*, *Staphylococcus aureus* ATCC25923; *B. subtilis*, *Bacillus subtilis*; *M. luteus*, *Micrococcus luteus* ATCC 4698; *E. Coli*, *Escherichia coli* DH52; *S. dysenteriae*, *Shigella dysenteriae*; *P. aeruginosa*, *Pseudomonas aeruginosa*; *P. vulgaris*, *Proteus vulgaris*; *C. albicans*, *Candida albicans*; *C. mycoderma*, *Candida mycoderma*.

Table 3
Log*P* values of compounds **5a**–**k**

Compds	**5a**	**5b**	**5c**	**5d**	**5e**	**5f**	**5g**	**5h**	**5i**	**5j**	**5 k**
Log*P*	−0.34 ± 0.01	0.50 ± 0.03	0.53 ± 0.01	0.51 ± 0.03	0.57 ± 0.02	0.48 ± 0.04	0.52 ± 0.02	0.55 ± 0.04	0.56 ± 0.01	0.54 ± 0.03	0.53 ± 0.02

2.3.3. Solubility and stability

The solubility of the target compounds **5a**–**k** was tested. Phosphate buffer (pH 7.5) was added to the tested samples, and the resulting suspension was equilibrated by sonication (10 min) and shaking at room temperature for 20 h, followed by centrifugation. The supernatant was analyzed by UV spectrometry to determine the concentration of samples in solution using a regression curve (Supplementary data).

The stability of the prepared compounds **5a**–**k** was determined by UV spectrometry (Supplementary data). The experimental results (Table 4) indicated that all the tested compounds **5a**–**k** were stable at the pH values (6.5–8.5) and temperatures (30–80 °C).

2.4. Binding discussion

2.4.1. UV–vis absorption spectral study

UV–vis absorption spectroscopic method is a convenient technique for measuring the structural change of protein and the formation of complex. The UV–vis absorption measurement to study the interaction of compound **5g** with HSA has been carried out and the results are shown in Figure 4. Two absorption peaks at 278 and 340 nm were observed, and the peak intensity increased with the addition of compound **5g**. The enhancement of absorbance intensity evidences the binding interaction of compound **5g** to HSA. This phenomenon might result from the slightly increased hydrophobicity of the microenvironment of Tryptophan (Trp-214) residue.[40]

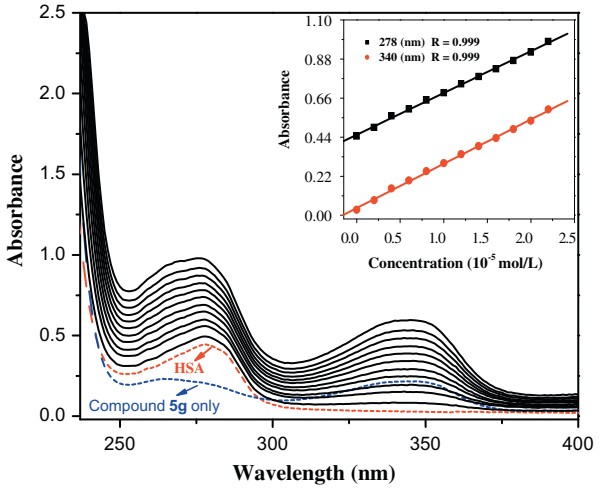

Figure 4. Effect of compound **5g** on the UV–vis absorption of HSA, c(HSA) = 1.0 × 10^{-5} mol/L; c(compound **5g**)/(10^{-5} mol/L): 0, 0.2, 0.4, 0.6, 0.8, 1, 1.2, 1.4, 1.6, 1.8, 2.0, 2.2 (T = 286 K, pH 7.40). The inset corresponds to the absorbance at 278 and 340 nm with different concentrations of compound **5g**.

2.4.2. Fluorescence quenching mechanism

Fluorescence quenching is considered as an effective approach to investigate the transportation ability of HSA to small molecules. Trp-214 is the only one tryptophan residue in HSA as fluorophore

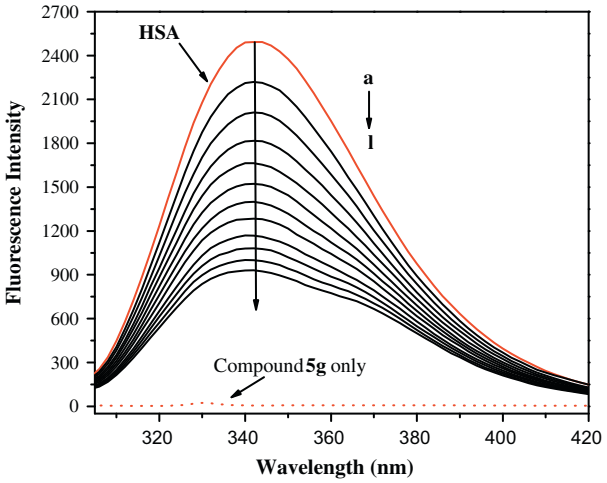

Figure 5. Emission spectra of HSA in the presence of various concentrations of compound **5g**. c(HSA) = 1.0 × 10^{-5} mol/L; c(compound **5g**)/(10^{-5} mol/L), *a–l*: from 0.0–2.2 at increments of 0.20; dash line shows the emission spectrum of compound **5g** only; T = 286 K, λ_{ex} = 295 nm.

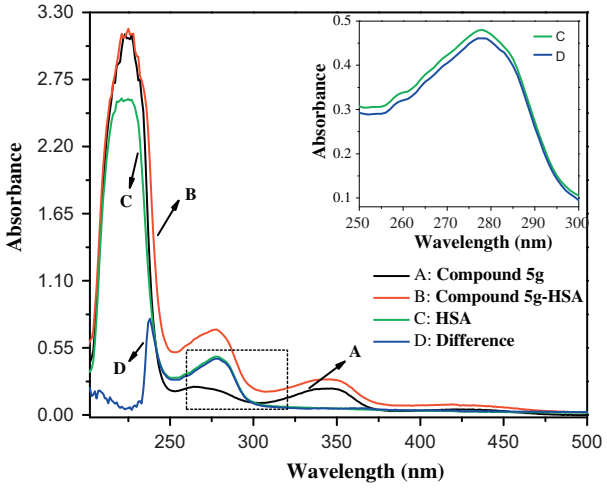

Figure 7. UV–vis spectra of HSA in the presence of compound **5g**: **A**, absorption spectrum of compound **5g** only; **B**, absorption spectrum of compound **5g**/HSA 1:1 complex; **C**, absorption spectrum of HSA only; **D**, difference between absorption spectrum of compound **5g**/HSA 1:1 complex and compound **5g**, c(HSA) = c(compound **5g**) = 1.0 × 10^{-5} M. The curves **C** and **D** for the wavelength ranging from 250–300 nm were depicted in the inset.

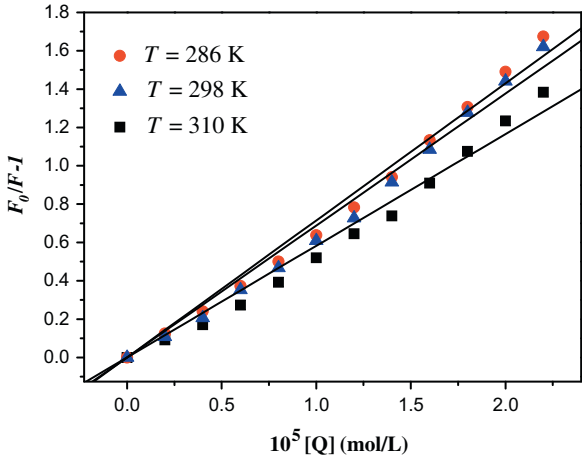

Figure 6. Stern–Volmer plots of compound **5g**-HSA system at three different temperatures.

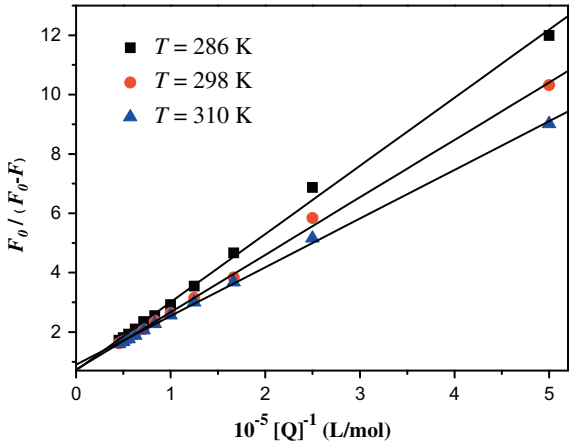

Figure 8. Modified Stern–Volmer plots.

capable of fluorescence quenching. The changed fluorescence intensity of Trp-214 resulted from the interaction of HSA with other small molecules could be reflected in the fluorescence spectra of HSA in the UV region.

The effect of compound **5g** on HSA fluorescence intensity at 286 K was shown in Figure 5. Evidently, a progressive decrease in the fluorescence intensity was caused by quenching, accompanied with the blue shift wavelength (from 342.8–339.8 nm) in the albumin spectrum. This suggested an increased hydrophobicity of the region surrounding the single Try-214 residue.[31]

The fluorescence quenching data can be analyzed by the well-known Stern–Volmer equation[41]:

$$\frac{F_0}{F} = 1 + K_{sv}[Q] \quad (1)$$

Table 5
Stern–Volmer quenching constants for the interaction of compound **5g** with HSA at various temperatures

pH	T (K)	$10^{-4}K_{SV}$ (L/mol)	R^a	SD[b]
7.4	295	3.325	0.999	0.024
	304	3.160	0.999	0.030
	310	3.080	0.998	0.031

[a] R is the correlation coefficient.
[b] SD is standard deviation.

where F_0 and F represent fluorescence intensities in the absence and presence of compound **5g**, respectively. K_{SV} is the Stern–Volmer quenching constant, and [Q] is the concentration of compound **5g**.

Table 4
Solubility of compounds **5a–k**

Compds	5a	5b	5c	5d	5e	5f	5g	5h	5i	5j	5k
Solubility (mg/L)	60.6	94.0	88.5	95.1	50.8	64.8	98.1	80.8	86.4	71.3	68.1

In order to verify the presence of static or dynamic quenching in compound **5g**-HSA complex, we have plotted F_0/F against Q and the results are shown in Figure 6.

The mechanisms of fluorescence quenching, often classified as dynamic quenching or static quenching were depended on temperature and viscosity. As higher temperatures lead to larger diffusion coefficients, the quenching constants are expected to increase with a gradually increasing temperature in dynamic quenching. Nevertheless, the increasing of temperature might induce a smaller static quenching constant due to the dissociation of weakly bound complexes.

The calculation of constant K_{SV} from Stern–Volmer plots (Table 5) demonstrated the effect on fluorescence quenching by compound **5g** at each temperature (295, 304, and 310 K) studied. The result showed that the Stern–Volmer quenching constant K_{SV} was inversely correlated with temperature, which manifested that the probable quenching mechanism of compound **5g**-HSA binding reaction was initiated by ground-state complex formation.[40]

The difference absorption spectroscopy was used to obtain spectra to reconfirm that the probable fluorescence quenching mechanism of HSA by compound **5g** was mainly initiated by ground-state complex formation. The UV–vis absorption spectrum of HSA and the difference absorption spectrum between HSA-compound **5g** complex and compound **5g** at the same concentration could not be superposed (Fig. 7), this result suggested that the probable quenching mechanism of fluorescence of HSA by compound **5g** was mainly a static quenching procedure.[31]

2.4.3. Binding constant and site

For a static quenching process, the data could be described by the modified Stern–Volmer equation[42]:

$$\frac{F_0}{\Delta F} = \frac{1}{f_a K_a}\frac{1}{[Q]} + \frac{1}{f_a} \tag{2}$$

where ΔF is the difference in fluorescence intensity in the absence and presence of compound **5g** at concentration [Q], f_a is the fraction of accessible fluorescence, and K_a is the effective quenching constant for the accessible fluorophores, which are analogous to associative binding constants for the quencher-acceptor system. The dependence of $F_0/\Delta F$ on the reciprocal value of quencher concentration $[Q]^{-1}$ is linear with the slope equaling to the value of $(f_a K_a)^{-1}$. The value $f_a{}^{-1}$ is fixed on the ordinate. The constant K_a is a quotient of the ordinate $f_a{}^{-1}$ and the slope $(f_a K_a)^{-1}$. The modified Stern–Volmer plots were Figure 8 and the calculated results were depicted in Table 6.

The numbers of binding sites and the equilibrium binding constants can also be calculated according to the Scatchard equation[43]:

$$r/D = nK_b - rK_b \tag{3}$$

where D_f is the molar concentration of free small molecules, r is the moles of small molecules bound per mole of protein, n is binding sites multiplicity per class of binding sites, and K_b is the equilibrium binding constant. The Scatchard plots (Supplementary data) and the K_b and n were listed in Table 6.

The results of the modified Stern–Volmer and Scatchard plots for the compound **5g-**HSA system at different temperatures were shown in Table 6. The decreasing trend of K_a and K_b with increasing temperatures was in accordance with K_{SV}'s dependence on temperatures. The value of binding sites n was approximately one, which indicated the interaction of compound **5g** with HSA seemed to be the presence of one high affinity binding site. The results also manifested that the binding constants were moderate and the effect of temperatures was not obvious, therefore compound **5g** might be stored and carried by HSA.

2.4.4. Binding mode and thermodynamic parameters

There are generally four kinds of noncovalent interactions like hydrogen bonds, van der Waals forces, electrostatic and hydrophobic bonds, which exert an important effect on small molecules binding to proteins.[44] The thermodynamic parameters enthalpy (ΔH) and entropy (ΔS) change of binding reaction are the main evidence for confirming the interactions between small molecules and protein. If the enthalpy change (ΔH) does not vary obviously over the studied temperatures range, then its value and that of entropy change (ΔS) can be evaluated from the van't Hoff equation:

$$\ln K = -\frac{\Delta H}{RT} + \frac{\Delta S}{R} \tag{4}$$

where K is analogous to the associative binding constants at the corresponding temperature and R is the gas constant. In order to explain the binding model between compound **5g** and HSA, the thermodynamic parameters were calculated from the van't Hoff plots. The enthalpy change (ΔH) was estimated from the slope of the van't Hoff relationship (Fig. 9). The free energy change (ΔG) was then calculated from the following equation:

$$\Delta G = \Delta H - T\Delta S \tag{5}$$

Table 7 summarized the values of ΔH, ΔG and ΔS. The negative values of free energy ΔG of the interaction between compound 5g and HSA suggested that the binding process was spontaneous, and

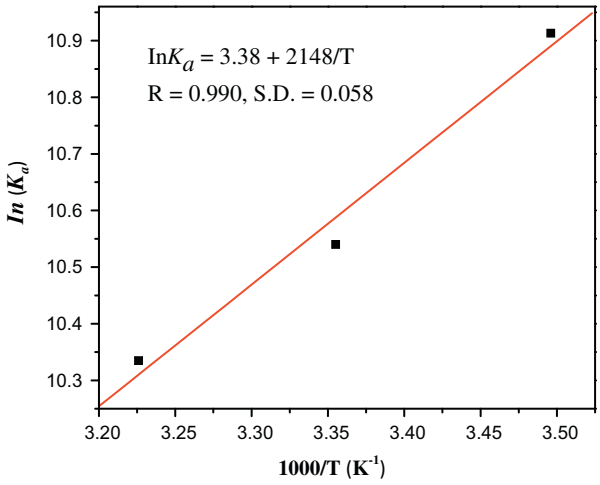

Figure 9. Van't Hoff plots of the compound **5g**-HSA system.

Table 6
Binding constants and sites of compound **5g**-HSA system at pH 7.4

T(K)	Modified Stern–Volmer Method	Scatchard Method			
	$10^{-4}K_a$ (L/mol)	$10^{-4}K_b$ (L/mol)	R	SD	n
286	5.49	5.08	0.994	0.009	1.17
298	3.78	3.80	0.997	0.005	1.37
310	3.08	3.02	0.996	0.005	1.46

Table 7
Thermodynamic parameters of compound **5g**-HSA system at different temperatures

T(K)	ΔH (kJ/mol)	ΔG (kJ/mol)	ΔS (J/mol K)
286		−25.89	
298	−17.86	−26.23	28.09
310		−26.58	

the negative values of enthalpy (ΔH) indicated that the binding was mainly enthalpy-driven and involved an exothermic reaction, the entropy (ΔS) was unfavorable for it. A positive (ΔS) value is frequently taken as a typical evidence for hydrophobic interaction, which is consistent with the above discussion. Therefore, enthalpy change ΔH < 0 and entropy change ΔS > 0 obtained in this case indicated that the electrostatic interactions played an important role in the binding of compound 5g to HSA (Table 7).[40]

3. Conclusions

In conclusion, a series of novel berberine nitroimidazoles was successfully synthesized by a convenient and efficient procedure starting from commercially available halobenzyl chlorides, diethanolamine and berberine. Their structures were confirmed by ^{1}H NMR, ^{13}C NMR, MS, IR and HRMS spectra. The in vitro antimicrobial evaluation revealed that most of the synthesized berberine nitroimidazoles could effectively inhibit the growth of the tested strains and some showed comparable or superior potency against *Methicillin-resistant S. aureus* to reference drugs Norfloxacin, Chloromycin and Berberine. Especially, nitroimidazole derivative **5g** with 2,4-difluorobenzyl moiety exhibited effective antibacterial and antifungal activities and particularly gave comparable or even better anti-Gram-negative (MIC = 4–8 μg/mL) and anti-*C. mycoderma* (MIC = 1 μg/mL) efficacies in comparison to reference drugs. Further transportation behavior of HSA to compound **5g** manifested that nitroimidazole **5g** could be effectively stored and carried by HSA. The experimental parameters indicated that the quenching mechanism of fluorescence of HSA by compound **5g** was a static quenching procedure. The association of compound **5g** with HSA was spontaneous and the electrostatic interactions played important roles in the transportation of HSA to **5g**.

4. Experimental

4.1. General methods

Melting points were recorded on X-6 melting point apparatus and uncorrected. TLC analysis was done using pre-coated silica gel plates. FT-IR spectra were carried out on Bruker RFS100/S spectrophotometer (Bio-Rad, Cambridge, MA, USA) using KBr pellets in the 400–4000 cm^{-1} range. NMR spectra were recorded on a Bruker AV 300 spectrometer using TMS as an internal standard. The chemical shifts were reported in parts per million (ppm), the coupling constants (*J*) were expressed in hertz (Hz) and signals were described as singlet (s), doublet (d), triplet (t), as well as multiplet (m). The following abbreviations were used to designate aryl groups: Im, nitroimidazolyl; Ph, phenyl; Ber, berberinyl. The mass spectra were recorded on LCMS-2010A and the high-resolution mass spectra (HRMS) were recorded on an IonSpec FT–ICR mass spectrometer with ESI resource. All fluorescence spectra were recorded on F-7000 Spectrofluorimeter (Hitachi, Tokyo, Japan) equipped with 1.0 cm quartz cells, the widths of both the excitation and emission slit were set as 2.5 nm, and the excitation wavelength was 295 nm. Fluorescence spectra were recorded at 286, 298, 310 K in the range of 300–450 nm. The UV spectrum was recorded at room temperature on a TU-2450 spectrophotometer (Puxi Analytic Instrument Ltd, of Beijing, China) equipped with 1.0 cm quartz cells. HSA was obtained from Sigma–Aldrich (St. Louis, MO, USA). Tris, NaCl and HCl were analytical purity. HSA was dissolved in Tris–HCl buffer solution (0.05 M Tris, 0.15 M NaCl, pH 7.4). Sample masses were weighed on a microbalance with a resolution of 0.1 mg. All other chemicals and solvents were commercially available, and were used without further purification.

4.1.1. General procedures for the HSA binding study

The concentration of HSA was fixed at 1.0×10^{-5} mol L^{-1} and that of compound **5g** was varied from 0 to 2.2×10^{-5} mol L^{-1} at increments of 0.2×10^{-5} mol L^{-1} in the fluorescence measurements. In the quenching experiments, the concentrations of HSA solution were stabilized at 1.0×10^{-5} mol L^{-1}, and solutions of compound **5g** with concentrations varied from 0 to 2.4×10^{-5} mol L^{-1} at increments of 0.2×10^{-5} mol L^{-1} were added to the HSA solution. Fluorescence spectra (λ_{ex} = 295 nm) were measured after the mixtures were incubated at 295, 304 and 310 K for 24 h, respectively.

4.1.2. General procedures for the preparation of intermediates diols (2a–e) and bromides (3a–e)

The intermediates **2a**–**e** and **3a**–**e** were prepared according to the previously reported methods.[27]

4.1.3. 2-Bromo-*N*-(2,4-difluorobenzyl)-*N*-[2-(2-methyl-5-nitro-1*H*-imidazol-1-yl)ethyl]ethanamine (4a)

A mixture of 2-methyl-5-nitroimidazole (1.29 g, 0.01 mol) and potassium carbonate (2.80 g, 0.02 mol) in acetonitrile (5 mL) was stirred at 60 °C for 1 h. After the mixture was cooled to room temperature, compound **3a** (4.20 g, 0.01 mol) was added and stirred for 2 h (monitored by TLC, eluent, ethyl acetate/petroleum, 1:2, v/v). After the solvent was evaporated under reduced pressure, and the resulting residue was extracted with ethyl acetate (3 × 30 mL), the organic layers were combined, dried over anhydrous sodium sulfate, and concentrated under reduced pressure. The crude product was purified by silica gel column chromatography eluting with ethyl acetate/petroleum (1:2, v/v) to afford the target compound **4a** (3.03 g) as white solid. Yield: 74.1%; mp: 107–108 °C; IR (KBr) *v*: 3085, 3067 (Ar–H), 2966, 2954, 2918, 2851 (CH_2, CH_3), 1602, 1535, 1499 (aromatic skeleton), 1420, 1327, 1289, 1234, 1137, 1049, 1031, 975, 853, 826 cm^{-1}; ^{1}H NMR (300 MHz, $CDCl_3$): δ 7.75 (s, 1H, Im 4-*H*), 7.20–6.76 (m, 3H, Ph 3,5,6-*H*), 3.93 (t, *J* = 6.2 Hz, 2H, Im-CH_2), 3.68 (s, 2H, PhCH_2), 3.38 (t, *J* = 6.0 Hz, 2H, Br–CH_2), 3.00 (t, *J* = 6.2 Hz, 2H, Im-CH_2CH_2), 2.89 (t, *J* = 6.0 Hz, 2H, Br–CH_2CH_2), 2.33 (s, 3H, Im-CH_3) ppm; MS (*m*/*z*): 404 [M+H]$^+$. HRMS (TOF) calcd for $C_{15}H_{17}BrF_2N_4O_2$: [M+H]$^+$, 404.2298; found, 404.2290.

4.1.4. 2-Bromo-*N*-(2,4-difluorobenzyl)-*N*-[2-(4-nitro-1*H*-imidazol-1-yl)ethyl]ethanamine (4b)

Compound **4b** was prepared according to the procedure described for compound **4a** starting from 4-nitroimidazole (1.70 g, 0.015 mol), potassium carbonate (4.25 g, 0.03 mol) and compound **3a** (5.52 g, 0.015 mol). The target compound **4b** (2.74 g) was obtained as white solid. Yield: 46.8%; mp: 101–102 °C; IR (KBr) *v*: 3072, 3014 (Ar–H), 2966, 2925, 2821 (CH_2), 1602, 1527, 1490 (aromatic skeleton), 1427, 1325, 1288, 1237, 1141, 1049, 1020, 984, 861, 820 cm^{-1}; ^{1}H NMR (300 MHz, $CDCl_3$): δ 7.71 (s, 1H, Im 5-*H*), 7.48 (s, 1H, Im 2-*H*), 7.16–6.79 (m, 3H, Ph 3,5,6-*H*), 4.06 (t, *J* = 6.2 Hz, 2H, Im-CH_2), 3.67 (s, 2H, PhCH_2), 3.38 (t, *J* = 6.0 Hz, 2H, Br–CH_2), 2.99 (t, *J* = 6.2 Hz, 2H, Im-CH_2CH_2), 2.90 (t, *J* = 6.0 Hz, 2H, Br–CH_2CH_2) ppm; MS (*m*/*z*): 390 [M+H]$^+$. HRMS (TOF) calcd for $C_{14}H_{15}BrF_2N_4O_2$: [M+H]$^+$, 390.2032; found, 390.2040.

4.1.5. 2-Bromo-*N*-(3,4-dichlorobenzyl)-*N*-[2-(4-nitro-1*H*-imidazol-1-yl)ethyl]ethanamine (4c)

Compound **4c** was prepared according to the procedure described for compound **4a** starting from 4-nitroimidazole (1.15 g, 0.01 mol), potassium carbonate (2.99 g, 0.02 mol) and compound **3b** (3.98 g, 0.01 mol). The target compound **4c** (2.37 g) was obtained as white solid. Yield: 55.4%; mp: 115–117 °C; IR (KBr) *v*: 3078, 3018 (Ar–H), 2971, 2953, 2825 (CH_2), 1595, 1523, 1482 (aromatic skeleton), 1410, 1327, 1285, 1229, 1124, 1051, 1029, 981,

865, 822 cm^{-1}; ^1H NMR (300 MHz, $CDCl_3$): δ 7.75 (s, 1H, Im 5-*H*), 7.47 (s, 1H, Im 2-*H*), 7.34–6.98 (m, 3H, Ph 2,5,6-*H*), 4.03 (t, *J* = 6.2 Hz, 2H, Im-CH_2), 3.69 (s, 2H, PhCH_2), 3.43 (t, *J* = 6.0 Hz, 2H, Br–CH_2), 3.02 (t, *J* = 6.2 Hz, 2H, Im-CH_2CH_2), 2.89 (t, *J* = 6.0 Hz, 2H, Br–CH_2CH_2) ppm; MS (*m*/*z*): 423 $[M+H]^+$. HRMS (TOF) calcd for $C_{14}H_{15}BrCl_2N_4O_2$: $[M+Na]^+$, 442.9653; found, 442.9651.

4.1.6. 2-Bromo-*N*-(2-chlorobenzyl)-*N*-[2-(4-nitro-1*H*-imidazol-1-yl)ethyl]ethanamine (4d)

Compound **4d** was prepared according to the procedure described for compound **4a** starting from 4-nitroimidazole (1.14 g, 0.01 mol), potassium carbonate (2.93 g, 0.02 mol) and compound **3c** (4.54 g, 0.013 mol). The target compound **4d** (2.92 g) was obtained as white solid. Yield: 75.0%; mp: 89–90 °C; IR (KBr) *v*: 3091, 3067 (Ar–H), 2923, 2843 (CH_2), 1593, 1519, 1485, 1435 (aromatic skeleton), 1371, 1286, 1223, 1126, 1053, 1033, 982, 874, 824 cm^{-1}; ^1H NMR (300 MHz, $CDCl_3$): δ 7.73 (s, 1H, Im 5-*H*), 7.52 (s, 1H, Im 2-*H*), 7.32–7.17 (m, 4H, Ph 3,4,5,6-*H*), 3.99 (t, *J* = 6.2 Hz, 2H, Im-CH_2), 3.76 (s, 2H, PhCH_2), 3.46 (t, *J* = 6.0 Hz, 2H, Br–CH_2), 3.07 (t, *J* = 6.2 Hz, 2H, Im-CH_2CH_2), 2.92 (t, *J* = 6.0 Hz, 2H, Br–CH_2CH_2) ppm; MS (*m*/*z*): 389 $[M+H]^+$. HRMS (TOF) calcd for $C_{14}H_{16}BrClN_4O_2$: $[M+Na]^+$, 409.0043; found, 409.0040.

4.1.7. 2-Bromo-*N*-(3-chlorobenzyl)-*N*-[2-(4-nitro-1*H*-imidazol-1-yl)ethyl]ethanamine (4e)

Compound **4e** was prepared according to the procedure described for compound **4a** starting from 4-nitroimidazole (1.12 g, 0.01 mol), potassium carbonate (3.00 g, 0.02 mol) and compound **3d** (3.96 g, 0.01 mol). The target compound **4e** (2.21 g) was obtained as white solid. Yield: 57.4%; mp: 68–69 °C; IR (KBr) *v*: 3068, 3021 (Ar–H), 2959, 2823 (CH_2), 1588, 1524, 1489, 1441 (aromatic skeleton), 1325, 1287, 1250, 1146, 1075, 1046, 983, 861, 822 cm^{-1}; ^1H NMR (300 MHz, $CDCl_3$): δ 7.69 (s, 1H, Im 5-*H*), 7.43 (s, 1H, Im 2-*H*), 7.24–7.01 (m, 4H, Ph 2,4,5,6-*H*), 3.98 (t, *J* = 6.2 Hz, 2H, Im-CH_2), 3.73 (s, 2H, PhCH_2), 3.43 (t, *J* = 6.0 Hz, 2H, Br–CH_2), 3.02 (t, *J* = 6.2 Hz, 2H, Im-CH_2CH_2), 2.87 (t, *J* = 6.0 Hz, 2H, Br–CH_2CH_2) ppm; MS (*m*/*z*): 389 $[M+H]^+$. HRMS (TOF) calcd for $C_{14}H_{16}BrClN_4O_2$: $[M+Na]^+$, 409.0043; found, 409.0041.

4.1.8. 2-Bromo-*N*-(4-chlorobenzyl)-*N*-[2-(4-nitro-1*H*-imidazol-1-yl)ethyl]ethanamine (4f)

Compound **4f** was prepared according to the procedure described for compound **4a** starting from 4-nitroimidazole (1.13 g, 0.01 mol), potassium carbonate (2.99 g, 0.02 mol) and compound **3e** (4.70 g, 0.013 mol). The target compound **4f** (3.09 g) was obtained as white solid. Yield: 80.0%; mp: 124–125 °C; IR (KBr) *v*: 3051 (Ar–H), 2962, 2822 (CH_2), 1597, 1516, 1491 (aromatic skeleton), 1427, 1371, 1272, 1234, 1144, 1050, 1017, 964, 857, 821 cm^{-1}; ^1H NMR (300 MHz, $CDCl_3$): δ 7.67 (s, 1H, Im 5-*H*), 7.45 (s, 1H, Im 2-*H*), 7.26–7.08 (m, 4H, Ph 2,3,5,6-*H*), 3.99 (t, *J* = 6.2 Hz, 2H, Im-CH_2), 3.70 (s, 2H, PhCH_2), 3.40 (t, *J* = 6.0 Hz, 2H, Br–CH_2), 3.00 (t, *J* = 6.2 Hz, 2H, Im-CH_2CH_2), 2.88 (t, *J* = 6.0 Hz, 2H, Br–CH_2CH_2) ppm. MS (*m*/*z*): 389 $[M+H]^+$. HRMS (TOF) calcd for $C_{14}H_{16}BrClN_4O_2$: $[M+Na]^+$, 409.0043; found, 409.0039.

4.1.9. 2-Bromo-*N*-(2,4-difluorobenzyl)-*N*-[2-(5-nitro-1*H*-imidazol-1-yl)ethyl]ethanamine (4g)

Compound **4g** was prepared according to the procedure described for compound **4a** starting from 4-nitroimidazole (1.70 g, 0.015 mol), potassium carbonate (4.25 g, 0.03 mol) and compound **3a** (5.52 g, 0.015 mol). The target compound **4g** (1.27 g) was obtained as white solid. Yield: 21.7%; IR (KBr) *v*: 3076, 3012 (Ar–H), 2967, 2923, 2823 (CH_2), 1603, 1519, 1497, 1421 (aromatic skeleton), 1326, 1280, 1239, 1143, 1051, 1023, 981, 864, 824 cm^{-1}; ^1H NMR (300 MHz, $CDCl_3$): δ 7.86 (s, 1H, Im 4-*H*), 7.69 (s, 1H, Im 2-*H*), 7.10–6.75 (m, 3H, Ph 3,5,6-*H*), 4.36 (t, *J* = 6.2 Hz, 2H, Im-CH_2), 3.73 (s, 2H, PhCH_2), 3.37 (t, *J* = 6.0 Hz, 2H, Br–CH_2), 2.98 (t, *J* = 6.2 Hz, 2H, Im-CH_2CH_2), 2.90 (t, *J* = 6.0 Hz, 2H, Br–CH_2CH_2) ppm; MS (*m*/*z*): 390 $[M+H]^+$. HRMS (TOF) calcd for $C_{14}H_{15}BrF_2N_4O_2$: $[M+H]^+$, 390.2032; found, 390.2030.

4.1.10. 2-Bromo-*N*-(3,4-dichlorobenzyl)-*N*-[2-(5-nitro-1*H*-imidazol-1-yl)ethyl]ethanamine (4h)

Compound **4h** was prepared according to the procedure described for compound **4a** starting from 4-nitroimidazole (1.15 g, 0.01 mol), potassium carbonate (2.99 g, 0.02 mol) and compound **3b** (3.98 g, 0.01 mol). The target compound **4h** (1.13 g) was obtained as white solid. Yield: 26.3%; IR (KBr) *v*: 3079, 3015 (Ar–H), 2974, 2950, 2822 (CH_2), 1594, 1522, 1487 (aromatic skeleton), 1415, 1323, 1286, 1227, 1128, 1054, 1025, 986, 869, 826 cm^{-1}; ^1H NMR (300 MHz, $CDCl_3$): δ 7.91 (s, 1H, Im 4-*H*), 7.67 (s, 1H, Im 2-*H*), 7.33–6.93 (m, 3H, Ph 2,5,6-*H*), 4.33 (t, *J* = 6.2 Hz, 2H, Im-CH_2), 3.75 (s, 2H, PhCH_2), 3.41 (t, *J* = 6.0 Hz, 2H, Br–CH_2), 3.00 (t, *J* = 6.2 Hz, 2H, Im-CH_2CH_2), 2.88 (t, *J* = 6.0 Hz, 2H, Br–CH_2CH_2) ppm; MS (*m*/*z*): 423 $[M+H]^+$. HRMS (TOF) calcd for $C_{14}H_{15}BrCl_2N_4O_2$: $[M+Na]^+$, 442.9653; found, 442.9650.

4.1.11. 2-Bromo-*N*-(2-chlorobenzyl)-*N*-[2-(5-nitro-1*H*-imidazol-1-yl)ethyl]ethanamine (4i)

Compound **4i** was prepared according to the procedure described for compound **4a** starting from 4-nitroimidazole (1.14 g, 0.01 mol), potassium carbonate (2.93 g, 0.02 mol) and compound **3c** (4.54 g, 0.013 mol). The target compound **4i** (1.06 g) was obtained as white solid. Yield: 26.9%; IR (KBr) *v*: 3095, 3068 (Ar–H), 2926, 2847 (CH_2), 1597, 1518, 1483, 1436 (aromatic skeleton), 1376, 1284, 1225, 1125, 1056, 1036, 984, 873, 821 cm^{-1}; ^1H NMR (300 MHz, $CDCl_3$): δ 7.84 (s, 1H, Im 4-*H*), 7.66 (s, 1H, Im 2-*H*), 7.29–7.14 (m, 4H, Ph 3,4,5,6-*H*), 4.39 (t, *J* = 6.2 Hz, 2H, Im-CH_2), 3.73 (s, 2H, PhCH_2), 3.41 (t, *J* = 6.0 Hz, 2H, Br–CH_2), 3.05 (t, *J* = 6.2 Hz, 2H, Im-CH_2CH_2), 2.94 (t, *J* = 6.0 Hz, 2H, Br–CH_2CH_2) ppm. MS (*m*/*z*): 388 $[M+H]^+$. HRMS (TOF) calcd for $C_{14}H_{16}BrClN_4O_2$: $[M+Na]^+$, 409.0043; found, 409.0041.

4.1.12. 2-Bromo-*N*-(3-chlorobenzyl)-*N*-[2-(5-nitro-1*H*-imidazol-1-yl)ethyl]ethanamine (4j)

Compound **4j** was prepared according to the procedure described for compound **4a** starting from 4-nitroimidazole (1.12 g, 0.01 mol), potassium carbonate (3.00 g, 0.02 mol) and compound **3d** (3.96 g, 0.01 mol). The target compound **4j** (0.87 g) was obtained as white solid. Yield: 22.6%; IR (KBr) *v*: 3066, 3020 (Ar-H), 2953, 2827 (CH_2), 1581, 1525, 1487, 1444 (aromatic skeleton), 1321, 1288, 1252, 1148, 1077, 1047, 988, 868, 823 cm^{-1}; ^1H NMR (300 MHz, $CDCl_3$): δ 7.90 (s, 1H, Im 4-*H*), 7.65 (s, 1H, Im 2-*H*), 7.24–6.97 (m, 4H, Ph 2,4,5,6-*H*), 4.31 (t, *J* = 6.2 Hz, 2H, Im-CH_2), 3.71 (s, 2H, PhCH_2), 3.40 (t, *J* = 6.0 Hz, 2H, Br–CH_2), 3.00 (t, *J* = 6.2 Hz, 2H, Im-CH_2CH_2), 2.88 (t, *J* = 6.0 Hz, 2H, Br–CH_2CH_2) ppm. MS (*m*/*z*): 388 $[M+H]^+$. HRMS (TOF) calcd for $C_{14}H_{16}BrClN_4O_2$: $[M+Na]^+$, 409.0043; found, 409.0040.

4.1.13. 2-Bromo-*N*-(4-chlorobenzyl)-*N*-[2-(5-nitro-1*H*-imidazol-1-yl)ethyl]ethanamine (4k)

Compound **4k** was prepared according to the procedure described for compound **4a** starting from 4-nitroimidazole (1.13 g, 0.01 mol), potassium carbonate (2.99 g, 0.02 mol) and compound **3e** (4.70 g, 0.013 mol). The target compound **4k** (0.73 g) was obtained as white solid. Yield: 18.5%; IR (KBr) *v*: 3049 (Ar-H), 2960, 2821 (CH_2), 1598, 1514, 1492 (aromatic skeleton), 1428, 1373, 1275, 1233, 1142, 1053, 1016, 962, 856, 820 cm^{-1}; ^1H NMR (300 MHz, $CDCl_3$): δ 7.92 (s, 1H, Im 4-*H*), 7.66 (s, 1H, Im 2-*H*), 7.35–7.18 (m, 4H, Ph 2,3,5,6-*H*), 4.32 (t, *J* = 6.2 Hz, 2H, Im-CH_2), 3.73 (s, 2H, PhCH_2), 3.32 (t, *J* = 6.0 Hz, 2H, Br–CH_2), 3.02 (t, *J* = 6.2 Hz, 2H, Im-CH_2CH_2), 2.98 (t, *J* = 6.0 Hz, 2H, Br–CH_2CH_2)

ppm; MS (*m*/*z*): 388 $[M+H]^+$. HRMS (TOF) calcd for $C_{14}H_{16}BrClN_4O_2$: $[M+H]^+$, 387.0223; found, 387.0214.

4.1.14. *N*-(2,4-Difluorobenzyl)-*N*-(2-(2-methyl-5-nitro-1*H*-imidazol-1-yl)ethyl)-2-(2-berberinoxyethoxy)ethanamine (5a)

To a stirred solution of berberrubine (1.39 g, 3.89 mmol) in DMF (10 mL), compound **4a** (1.60 g, 3.97 mmol) in DMF (5 mL) was added dropwise. The reaction mixture was then heated at 110 °C for 20 h. After the reaction was completed (monitored by TLC, eluent, chloroform/methanol, 20:1, v/v), the mixture was extracted with chloroform (3 × 30 mL). The organic layer was washed with water and dried over anhydrous sodium sulfate. After the filtrate was concentrated under reduced pressure, the crude product was purified by silica gel column chromatography eluting with chloroform/methanol (20:1, v/v) to afford the target compound **5a** (891 mg) as yellow solid. Yield: 33.7%; mp: 197–199 °C; IR (KBr) *v*: 3039 (Ar–H), 2949, 2846 (CH_2, CH_3), 1600, 1536, 1504, 1477 (aromatic skeleton), 1385, 1335, 1272, 1227, 1116, 1022, 933, 829 cm^{-1}; ^1H NMR (300 MHz, CD_3OD): δ 9.60 (s, 1H, Ber 8-*H*), 8.75 (s, 1H, Ber 13-*H*), 8.09 (d, *J* = 9.0 Hz, 1H, Ber 12-*H*), 7.72 (s, 1H, Im 4-*H*), 7.97 (d, *J* = 9.0 Hz, 1H, Ber 11-*H*), 7.63 (s, 1H, Ber 1-*H*), 7.30–7.27 (m, 1H, Ph 3-*H*), 7.14 (br, 1H, Ph 3-*H*), 7.04 (s, 1H, Ber 4-*H*), 6.94 (br, 1H, Ph 5-*H*), 6.14 (s, 2H, OCH_2O), 4.91 (br, 2H, Ber 6-*H*), 4.32 (t, *J* = 6.0 Hz, 2H, OCH_2CH_2N), 4.10 (t, *J* = 6.2 Hz, 2H, Im-CH_2), 4.02 (s, 3H, OCH_3), 3.80 (s, 2H, Ph–CH_2), 3.23 (br, 2H, Ber 5-*H*), 3.09 (t, *J* = 6.0 Hz, 2H, OCH_2CH_2N), 2.91 (t, *J* = 6.2 Hz, 2H, Im-CH_2CH_2), 2.28 (s, 3H, Im-CH_3) ppm; ^{13}C NMR (75 MHz, CD_3OD): δ 163.5, 163.4, 161.2, 161.1, 161.0, 159.1, 158.3, 150.1, 148.5, 146.9, 145.7, 145.2, 142.5, 142.1, 137.5, 135.7, 133.4, 132.9, 132.4, 131.1, 123.0, 121.6, 120.9, 119.6, 119.2, 118.9, 118.6, 118.2, 117.9, 111.9, 111.5, 108.9, 104.3, 104.1, 103.8, 102.5, 72.2, 57.4, 57.0, 53.0, 51.5, 46.0, 28.0, 26.9, 22.2 ppm; MS (*m*/*z*): 664 $[M-Cl]^+$; HRMS (TOF) calcd for $C_{34}H_{32}ClF_2N_5O_6$: $[M-Cl]^+$, 664.2315; found, 664.2319.

4.1.15. *N*-(2,4-Difluorobenzyl)-*N*-(2-(4-nitro-1*H*-imidazol-1-yl)ethyl)-2-(2-berberinoxyethoxy)ethanamine (5b)

Compound **5b** was prepared according to the procedure described for compound **5a** starting from berberrubine (1.83 g, 5.12 mmol) and compound **4b** (661 mg, 1.92 mmol). The target compound **5b** (784 mg) was obtained as yellow solid. Yield: 23.0%; mp: 198–200 °C; IR (KBr) *v*: 3074 (Ar–H), 2923, 2847 (CH_2, CH_3), 1601, 1541, 1504, 1483 (aromatic skeleton), 1383, 1345, 1272, 1224, 1100, 1033, 979, 846 cm^{-1}; ^1H NMR (300 MHz, CD_3OD): δ 9.55 (s, 1H, Ber 8-*H*), 8.74 (s, 1H, Ber 13-*H*), 7.84 (s, 1H, Im 5-*H*), 8.17 (d, *J* = 9.0 Hz, 1H, Ber 12-*H*), 7.96 (d, *J* = 9.0 Hz, 1H, Ber 11-*H*), 7.62 (s, 1H, Ber 1-*H*), 7.51 (s, 1H, Im 2-*H*), 7.30–6.94 (m, 3H, Ph 3,5,6-*H*), 6.95 (s, 1H, Ber 4-*H*), 6.12 (s, 2H, OCH_2O), 4.95 (br, 2H, Ber 6-*H*), 4.38 (t, *J* = 6.0 Hz, 2H, OCH_2CH_2N), 4.02 (s, 3H, OCH_3), 4.01 (t, *J* = 6.2 Hz, 2H, Im-CH_2), 3.80 (s, 2H, Ph–CH_2), 3.23 (br, 2H, Ber 5-*H*), 3.03 (t, *J* = 6.0 Hz, 2H, OCH_2CH_2N), 2.95 (t, *J* = 6.0 Hz, 2H, Im-CH_2CH_2) ppm; ^{13}C NMR (75 MHz, CD_3OD): δ 164.1, 163.8, 161.7, 161.6, 161.5, 161.2, 159.0, 158.1, 151.5, 148.2, 146.4, 145.8, 145.1, 143.5, 142.9, 139.4, 135.3, 133.6, 132.3, 132.2, 131.1, 125.4, 123.0, 120.9, 119.4, 119.3, 118.9, 118.6, 118.2, 117.9, 112.0, 111.8, 108.9, 104.6, 104.2, 103.8, 102.5, 72.2, 57.1, 54.5, 52.6, 51.8, 46.7, 27.7, 26.4 ppm; MS (*m*/*z*): 630 $[M-Cl]^+$; HRMS (TOF) calcd for $C_{33}H_{30}ClF_2N_5O_6$: $[M-Cl]^+$, 630.2159; found, 630.2154.

4.1.16. *N*-(3,4-Dichlorobenzyl)-*N*-(2-(4-nitro-1*H*-imidazol-1-yl)ethyl)-2-(2-berberinoxyethoxy)ethanamine (5c)

Compound **5c** was prepared according to the procedure described for compound **5a** starting from berberrubine (1.27 g, 3.55 mmol) and compound **4c** (1.50 g, 3.55 mmol). The target compound **5c** (648 mg) was obtained as yellow solid. Yield: 26.1%; mp: 194–195 °C; IR (KBr) *v*: 3075, 3011 (Ar–H), 2923, 2851 (CH_2, CH_3), 1601, 1542, 1506, 1483 (aromatic skeleton), 1386, 1346, 1272, 1230, 1138, 1064, 981, 821 cm^{-1}; ^1H NMR (300 MHz, CD_3OD): δ 9.61 (s, 1H, Ber 8-*H*), 8.75 (s, 1H, Ber 13-*H*), 7.84 (s, 1H, Im 5-*H*), 8.10 (d, 1H, *J* = 9 Hz, Ber 12-*H*), 7.99 (d, 1H, *J* = 9 Hz, Ber 11-*H*), 7.71 (s, 1H, Ber 1-*H*), 7. 46 (s, 1H, Im 2-*H*), 7.47–7.14 (m, 3H, Ph 2,5,6-*H*), 7.01 (s, 1H, Ber 4-*H*), 6.08 (s, 2H, OCH_2O), 4.93 (br, 2H, Ber 6-*H*), 4.31 (t, *J* = 6.0 Hz, 2H, OCH_2CH_2N), 4.08 (t, *J* = 6.2 Hz, 2H, Im-CH_2), 4.04 (s, 3H, OCH_3), 3.77 (s, 2H, Ph–CH_2), 3.23 (br, 2H, Ber 5-*H*), 3.08 (t, *J* = 6.0 Hz, 2H, OCH_2CH_2N), 2.91 (t, *J* = 6.2 Hz, 2H, Im-CH_2CH_2) ppm; ^{13}C NMR (75 MHz, CD_3OD): δ 151.4, 148.7, 146.8, 146.7, 146.1, 144.7, 142.8, 139.4, 136.5, 133.2, 133.1, 132.6, 131.7, 130.2, 128.6, 125.4, 124.1, 123.3, 121.2, 119.5, 118.7, 118.2, 117.5, 108.4, 102.9, 72.5, 57.3, 54.2, 53.0, 51.5, 46.0, 28.0, 26.1 ppm; MS (*m*/*z*): 663 $[M-Cl]^+$; HRMS (TOF) calcd for $C_{33}H_{30}Cl_3N_5O_6$: $[M-Cl]^+$, 662.1568; found, 662.1574.

4.1.17. *N*-(2-Chlorobenzyl)-*N*-(2-(4-nitro-1*H*-imidazol-1-yl)ethyl)-2-(2-berberinoxyethoxy)ethanamine (5d)

Compound **5d** was prepared according to the procedure described for compound **5a** starting from berberrubine (1.07 g, 2.99 mmol) and compound **4d** (1.18 g, 3.04 mmol). The target compound **5d** (528 mg) was obtained as yellow solid. Yield: 26.6%; mp: 169–170 °C. IR (KBr) *v*: 3064 (Ar–H), 2957, 2843 (CH_2, CH_3), 1599, 1537, 1504, 1479 (aromatic skeleton), 1384, 1344, 1273, 1230, 1102, 1034, 926, 823 cm^{-1}; ^1H NMR (300 MHz, CD_3OD): δ 9.62 (s, 1H, Ber 8-*H*), 8.67 (s, 1H, Ber 13-*H*), 7.83 (s, 1H, Im 5-*H*), 8.11 (d, 1H, *J* = 9 Hz, Ber 12-*H*), 7.98 (d, 1H, *J* = 9 Hz, Ber 11-*H*), 7.72 (s, 1H, Ber 1-*H*), 7.44 (s, 1H, Im 2-*H*), 7.11–6.88 (m, 4H, Ph 3,4,5,6-H), 6.11 (s, 2H, OCH_2O), 5.46 (br, 2H, Ber 6-*H*), 4.05 (t, *J* = 6.2 Hz, 2H, Im-CH_2), 4.31 (t, *J* = 6.0 Hz, 4H, OCH_2CH_2N), 4.03 (s, 3H, OCH_3), 3.68 (s, 2H, Ph–CH_2), 3.50 (br, 2H, Ber 5-*H*), 3.05 (t, *J* = 6.0 Hz, 2H, OCH_2CH_2N), 3.09 (t, *J* = 6.2 Hz, 2H, Im-CH_2CH_2) ppm; ^{13}C NMR (75 MHz, CD_3OD): δ 151.1, 149.3, 147.7, 145.4, 145.3, 144.9, 142.9, 139.3, 133.6, 133.4, 132.2, 131.1, 129.6, 128.8, 127.2, 126.6, 125.4, 123.0, 120.9, 118.9, 118.6, 118.2, 117.9, 108.9, 102.5, 72.2, 57.4, 54.5, 53.8, 51.1, 46.4, 28.2, 26.8 ppm; MS (*m*/*z*): 628 $[M-Cl]^+$. HRMS (TOF) calcd for $C_{33}H_{31}Cl_2N_5O_6$: $[M-Cl]^+$, 629.1957; found, 629.1954.

4.1.18. *N*-(3-Chlorobenzyl)-*N*-(2-(4-nitro-1*H*-imidazol-1-yl)ethyl)-2-(2-berberinoxyethoxy)ethanamine (5e)

Compound **5e** was prepared according to the procedure described for compound **5a** starting from berberrubine (1.77 g, 4.95 mmol) and compound **4e** (1.71 g, 4.98 mmol). The target compound **5e** (1.38 g) was obtained as yellow solid. Yield: 34.7%; mp: 157–158 °C; IR (KBr) *v*: 3031 (Ar-H), 2968, 2844 (CH_2, CH_3), 1601, 1534, 1505, 1479 (aromatic skeleton), 1386, 1348, 1274, 1228, 1099, 1040, 941, 871 cm^{-1}; ^1H NMR (300 MHz, CD_3OD): δ 9.62 (s, 1H, Ber 8-*H*), 8.22 (s, 1H, Ber 13-*H*), 8.19 (s, 1H, Im 5-*H*), 7.87–7.79 (m, 2H, 11, Ber 12-*H*), 7.53 (s, 1H, Im 2-*H*), 7.35 (s, 1H, Ber 1-*H*), 7.17–7.11 (m, 3H, Ph 2,5,6-*H*), 6.85 (s, 1H, Ber 4-*H*), 6.11 (s, 2H, OCH_2O), 4.96 (br, 2H, Ber 6-*H*), 4.53 (t, *J* = 6.0 Hz, 2H, OCH_2CH_2N), 4.04 (t, *J* = 6.2 Hz, 2H, Im-CH_2), 3.98 (s, 3H, OCH_3), 3.72 (s, 2H, Ph–CH_2), 3.29 (br, 2H, Ber 5-*H*), 3.07 (t, *J* = 6.0 Hz, 2H, OCH_2CH_2N), 2.92 (t, *J* = 6.2 Hz, 2H, Im-CH_2CH_2) ppm; ^{13}C NMR (75 MHz, CD_3OD): δ 150.5, 149.3, 146.5, 146.3, 145.9, 143.5, 141.9, 139.5, 138.1, 134.8, 133.4, 131.1, 130.1, 126.6, 125.4, 124.1, 123.0, 120.9, 119.8, 119.1, 118.6, 117.9, 112.5, 108.9, 102.5, 72.4, 57.7, 54.1, 53.4, 51.6, 45.6, 28.1, 27.4 ppm; MS (*m*/*z*): 628 $[M-Cl]^+$; HRMS (TOF) calcd for $C_{33}H_{31}Cl_2N_5O_6$: $[M-Cl]^+$, 629.1957; found, 629.1953.

4.1.19. *N*-(4-Chlorobenzyl)-*N*-(2-(4-nitro-1*H*-imidazol-1-yl)ethyl)-2-(2-berberinoxyethoxy)ethanamine (5f)

Compound **5f** was prepared according to the procedure described for compound **5a** starting from berberrubine (1.06 g,

2.96 mmol) and compound **4f** (1.30 g, 3.35 mmol). The target compound **5f** (624 mg) was obtained as yellow solid. Yield: 31.8%; mp: 205–206 °C; IR (KBr) *v*: 3066 (Ar–H), 2972, 2819 (CH_2, CH_3), 1600, 1542, 1522, 1483 (aromatic skeleton), 1384, 1345, 1271, 1223, 1101, 1033, 932, 821 cm^{-1}; ^1H NMR (300 MHz, CD_3OD): δ 9.61 (s, 1H, Ber 8-*H*), 8.72 (s, 1H, Ber 13-*H*), 7.83 (s, 1H, Im 5-*H*), 8.05 (d, *J* = 9 Hz, 1H, Ber 12-*H*), 7.97 (d, *J* = 9 Hz, 1H, Ber 12-*H*), 7.64 (s, 1H, Ber 1-*H*), 7.45 (s, 1H, Im 2-*H*), 7.21–6.92 (m, 5H, 4-*H*, Ph 2,3,5,6-*H*), 6.12 (s, 2H, OCH_2O), 4.95 (br, 2H, Ber 6-*H*), 4.48 (t, *J* = 6.0 Hz, 2H, OCH_2CH_2N), 4.08 (t, *J* = 6.0 Hz, 2H, Im-CH_2), 4.03 (s, 3H, OCH_3), 3.73 (s, 2H, Ph-CH_2), 3.26 (br, 2H, Ber 5-*H*), 2.97 (t, *J* = 6.0 Hz, 4H, OCH_2CH_2N, Im-CH_2CH_2) ppm; ^{13}C NMR (75 MHz, CD_3OD): δ 150.4, 148.2, 146.7, 146.1, 145.7, 144.1, 143.3, 139.1, 134.5, 133.6, 133.4, 131.1, 129.1, 127.7, 125.4, 123.0, 120.2, 119.6, 118.7, 118.4, 116.1, 108.9, 102.5, 72.2, 57.4, 55.3, 54.4, 52.3, 47.3, 28.2, 27.6 ppm; MS (*m*/*z*): 628 $[M-Cl]^+$; HRMS (TOF) calcd for $C_{33}H_{31}Cl_2N_5O_6$: $[M-Cl]^+$, 629.1957; found, 629.1948.

4.1.20. *N*-(2,4-Difluorobenzyl)-*N*-(2-(5-nitro-1*H*-imidazol-1-yl)ethyl)-2-(2-berberinoxyethoxy)ethanamine (5g)

Compound **5g** was prepared according to the procedure described for compound **5a** starting from berberrubine (1.92 g, 5.36 mmol) and compound **4g** (2.09 g, 5.37 mmol). The target compound **5g** (907 mg) was obtained as yellow solid. Yield: 25.4%; mp: 201–203 °C; IR (KBr) *v*: 3053 (Ar–H), 2922, 2850 (CH_2, CH_3), 1601, 1568, 1506, 1474 (aromatic skeleton), 1368, 1341, 1270, 1230, 1117, 1035, 931, 824 cm^{-1}; ^1H NMR (300 MHz, CD_3OD): δ 9.64 (s, 1H, Ber 8-*H*), 8.76 (s, 1H, Ber 13-*H*), 7.79 (s, 1H, Im 4-*H*), 8.05 (d, *J* = 9.0 Hz, 1H, Ber 12-*H*), 7.98 (d, *J* = 9.0 Hz, 1H, Ber 11-*H*), 7.64 (s, 1H, Im 2-*H*), 7.64 (s, 1H, Ber 1-*H*), 7.23–6.91 (m, 4H, 4-*H*, Ph 3,5,6-*H*), 6.11 (s, 2H, OCH_2O), 4.94 (br, 2H, Ber 6-*H*), 4.37 (t, *J* = 6.0 Hz, 2H, OCH_2CH_2N), 4.32 (t, *J* = 6.2 Hz, 2H, Im-CH_2), 4.04 (s, 3H, OCH_3), 3.77 (s, 2H, Ph-CH_2), 3.25 (br, 2H, Ber 5-*H*), 3.09 (t, *J* = 6.0 Hz, 2H, OCH_2CH_2N), 2.91 (t, *J* = 6.2 Hz, 2H, Im-CH_2CH_2) ppm; ^{13}C NMR (75 MHz, CD_3OD): δ 163.7, 163.3, 162.1, 161.5, 161.0, 160.6, 159.3, 158.4, 152.1, 147.7, 146.2, 145.9, 144.3, 143.0, 142.9, 136.0, 135.2, 133.4, 132.3, 132.1, 131.1, 126.0, 123.0, 120.9, 119.4, 119.2, 118.9, 118.6, 118.2, 117.9, 111.5, 108.9, 104.3, 104.1, 103.8, 102.1, 72.3, 58.4, 57.1, 53.2, 51.4, 46.2, 28.5, 27.3 ppm; MS (*m*/*z*): 631 $[M-Cl]^+$; HRMS (TOF) calcd for $C_{33}H_{30}ClF_2N_5O_6$: $[M-Cl]^+$, 630.2159; found, 630.2156.

4.1.21. *N*-(3,4-Dichlorobenzyl)-*N*-(2-(5-nitro-1*H*-imidazol-1-yl)ethyl)-2-(2-berberinoxyethoxy)ethanamine (5h)

Compound **5h** was prepared according to the procedure described for compound **5a** starting from berberrubine (1.90 g, 4.50 mmol) and compound **4h** (1.59 g, 4.44 mmol). The target compound **5h** (851 mg) was obtained as yellow solid. Yield: 27.1%; mp: 185–187 °C; IR (KBr) *v*: 3018 (Ar–H), 2922, 2850 (CH_2, CH_3), 1601, 1570, 1506, 1475 (aromatic skeleton), 1367, 1342, 1273, 1231, 1117, 1102, 1036, 975, 825 cm^{-1}; ^1H NMR (300 MHz, CD_3OD): δ 9.59 (s, 1H, Ber 8-*H*), 8.75 (s, 1H, Ber 13-*H*), 8.05 (d, *J* = 9.0 Hz, 1H, Ber 12-*H*), 7.98 (d, *J* = 9.0 Hz, 1H, Ber 11-*H*), 7.88 (s, 1H, Im 4-*H*), 7.71 (s, 1H, Im 2-*H*), 7.67 (s, 1H, Ber 1-*H*), 7.45 (br, 1H, Ph 5-*H*), 7.20–7.11 (m, 2H, Ph 2,6-*H*), 6.95 (s, 1H, Ber 4-*H*), 6.13 (s, 2H, OCH_2O), 4.92 (br, 2H, Ber 6-*H*), 4.41 (t, *J* = 6.0 Hz, 2H, OCH_2CH_2N), 4.35 (t, *J* = 6.2 Hz, 2H, Im-CH_2), 4.03 (s, 3H, OCH_3), 3.74 (s, 2H, Ph–CH_2), 3.22 (br, 2H, Ber 5-*H*), 3.10 (t, *J* = 6.0 Hz, 2H, OCH_2CH_2N), 2.90 (t, *J* = 6.2 Hz, 2H, Im-CH_2CH_2) ppm; ^{13}C NMR (75 MHz, CD_3OD): δ 150.5, 148.4, 145.7, 145.4, 145.2, 143.6, 143.2, 136.4, 136.0, 133.4, 133.1, 132.2, 131.3, 130.8, 128.5, 126.0, 125.3, 123.0, 120.9, 119.4, 118.8, 118.1, 116.5, 108.9, 102.5, 72.2, 58.6, 57.2, 53.3, 51.2, 46.1, 28.3, 27.2 ppm; MS (*m*/*z*): 663 $[M-Cl]^+$. HRMS (TOF) calcd for $C_{33}H_{30}Cl_3N_5O_6$: $[M-Cl]^+$, 662.1568; found, 662.1563.

4.1.22. *N*-(2-Chlorobenzyl)-*N*-(2-(5-nitro-1*H*-imidazol-1-yl)ethyl)-2-(2-berberinoxyethoxy)ethanamine (5i)

Compound **5i** was prepared according to the procedure described for compound **5a** starting from berberrubine (0.89 g, 2.49 mmol) and compound **4i** (0.94 g, 2.43 mmol). The pure compound **5i** (639 mg) was obtained as yellow solid. Yield: 38.7%; mp: 231–233 °C; IR (KBr) *v*: 3133, 3078 (Ar–H), 2955, 2824 (CH_2, CH_3), 1600, 1528, 1507, 1475 (aromatic skeleton), 1383, 1349, 1276, 1235, 1102, 1065, 937, 854 cm^{-1}; ^1H NMR (300 MHz, CD_3OD): δ 9.55 (s, 1H, Ber 8-*H*), 8.68 (s, 1H, Ber 13-*H*), 7.88 (s, 1H, Im 4-*H*), 8. 04 (d, *J* = 9.0 Hz, 1H, Ber 11-*H*), 7. 97 (d, *J* = 9.0 Hz, 2H, Ber 12-*H*), 7.64 (s, 1H, Im 2-*H*), 7.17–7.12 (m, 4H, Ph 3,4,5-H), 7.63 (s, 1H, Ber 1-*H*), 6.85 (s, 1H, Ph 6-*H*), 6.11 (s, 2H, OCH_2O), 4.98 (br, 2H, Ber 6-*H*), 4.41 (t, *J* = 6.0 Hz, 2H, OCH_2CH_2N), 4.32 (t, *J* = 6.2 Hz, 2H, Im-CH_2), 3.99 (s, 3H, OCH_3), 3.75 (s, 2H, Ph–CH_2), 3.34 (br, 2H, Ber 5-*H*), 3.07 (t, *J* = 6.0 Hz, 2H, OCH_2CH_2N), 2.97 (t, *J* = 6.2 Hz, 2H, Im-CH_2CH_2) ppm; ^{13}C NMR (75 MHz, CD_3OD): δ 150.4, 148.0, 146.4, 145.7, 144.6, 143.2, 142.1, 136.5, 133.4, 133.0, 132.1, 131.1, 129.4, 128.8, 127.1, 126.6, 125.3, 123.0, 120.9, 119.3, 118.7, 118.1, 116.4, 108.2, 102.4, 72.2, 58.6, 57.3, 53.2, 51.2, 46.6, 29.2, 27.3 ppm; MS (*m*/*z*): 628 $[M-Cl]^+$. HRMS (TOF) calcd for $C_{33}H_{31}Cl_2N_5O_6$: $[M-Cl]^+$, 628.1957; found, 628.1963.

4.1.23. *N*-(3-Chlorobenzyl)-*N*-(2-(5-nitro-1*H*-imidazol-1-yl)ethyl)-2-(2-berberinoxyethoxy)ethanamine (5j)

Compound **5j** was prepared according to the procedure described for compound **5a** starting from berberrubine (0.89 g, 2.49 mmol) and compound **4j** (0.85 g, 2.47 mmol). The pure compound **5j** (554 mg) was obtained as yellow solid. Yield: 33.5%; mp: 227–229 °C; IR (KBr) *v*: 3023 (Ar–H), 2969, 2816 (CH_2, CH_3), 1600, 1534, 1505, 1477 (aromatic skeleton), 1371, 1350, 1270, 1229, 1101, 1037, 928, 869 cm^{-1}; ^1H NMR (300 MHz, CD_3OD): δ 9.59 (s, 1H, Ber 8-*H*), 8.69 (s, 1H, Ber 13-*H*), 8. 04 (d, *J* = 9.0 Hz, 1H, Ber 11-*H*), 7. 97 (d, *J* = 9.0 Hz, 2H, Ber 12-*H*), 7.89 (s, 1H, Im 4-*H*), 7.65 (s, 1H, Im 2-*H*), 7.70 (s, 1H, Ber 1-*H*), 7.16–7.02 (m, 3H, Ph 2,5,6-*H*), 6.96 (s, 1H, Ber 4-*H*), 6.12 (s, 2H, OCH_2O), 4.91 (br, 2H, Ber 6-*H*), 4.41 (t, *J* = 6.0 Hz, 2H, OCH_2CH_2N), 4.37 (t, *J* = 6.2 Hz, 2H, Im-CH_2), 4.05 (s, 3H, OCH_3), 3.76 (s, 2H, Ph–CH_2), 3.31 (br, 2H, Ber 5-*H*), 3.09 (t, *J* = 6.0 Hz, 2H, OCH_2CH_2N), 2.89 (t, *J* = 6.0 Hz, 2H, Im-CH_2CH_2) ppm; ^{13}C NMR (75 MHz, CD_3OD): δ 150.6, 148.3, 145.7, 145.3, 145.1, 143.5, 143.2, 138.3, 136.2, 134.0, 133.4, 131.1, 130.4, 126.8, 126.0, 124.1, 123.5, 121.3, 118.9, 118.4, 117.9, 117.3, 112.4, 109.5, 102.6, 72.4, 58.9, 57.8, 52.6, 51.3, 45.7, 27.8, 26.7 ppm; MS (*m*/*z*): 628 $[M-Cl]^+$; HRMS (TOF) calcd for $C_{33}H_{31}Cl_2N_5O_6$: $[M-Cl]^+$, 628.1957; found, 628.1954.

4.1.24. *N*-(4-Chlorobenzyl)-*N*-(2-(5-nitro-1*H*-imidazol-1-yl)ethyl)-2-(2-berberinoxyethoxy)ethanamine (5k)

Compound **5k** was prepared according to the procedure described for compound **5a** starting from berberrubine (0.55 g, 1.54 mmol) and compound **4k** (0.60 g, 1.55 mmol). The target compound **5k** (310 mg) was obtained as yellow solid. Yield: 30.3%; mp: 173–174 °C; IR (KBr) *v*: 3044 (Ar–H), 2922, 2845 (CH_2, CH_3), 1600, 1542, 1506, 1479 (aromatic skeleton), 1384, 1347, 1273, 1230, 1101, 1038, 937, 825 cm^{-1}; ^1H NMR (300 MHz, CD_3OD): δ 9.57 (s, 1H, Ber 8-*H*), 8.73 (s, 1H, Ber 13-*H*), 7.84 (s, 1H, Im 4-*H*), 8.06 (d, *J* = 9.0 Hz, 1H, Ber 12-*H*), 7.96 (d, *J* = 9.0 Hz, 1H, Ber 11-*H*), 7.71 (s, 1H, Im 2-*H*), 7.67 (s, 1H, Ber 1-*H*), 7.24–7.17 (m, 4H, Ph 2,3,5,6-*H*), 6.95 (s, 1H, Ber 4-*H*), 6.13 (s, 2H, OCH_2O), 4.87 (br, 2H, Ber 6-*H*), 4.39 (t, *J* = 6.0 Hz, 2H, OCH_2CH_2N), 4.34 (t, *J* = 6.2 Hz, 2H, Im-CH_2), 4.05 (s, 3H, OCH_3), 3.68 (s, 2H, Ph–CH_2), 3.19 (br, 2H, Ber 5-*H*), 3.09 (t, *J* = 6.0 Hz, 2H, OCH_2CH_2N), 2.91 (t, *J* = 6.2 Hz, 2H, Im-CH_2CH_2) ppm; ^{13}C NMR (75 MHz, CD_3OD): δ 150.6, 148.3, 145.7, 145.5, 145.2, 142.8, 142.2, 136.4, 134.5, 133.7, 133.4,

131.1, 129.1, 127.7, 126.0, 123.4, 121.2, 119.3, 118.7, 118.2, 117.9, 108.3, 102.6, 72.3, 58.0, 57.1, 54.2, 51.3, 45.8, 28.3, 27.0 ppm; MS (m/z): 628 $[M-Cl]^+$; HRMS (TOF) calcd for $C_{33}H_{31}Cl_2N_5O_6$: $[M-Cl]^+$, 628.1957; found, 628.1949.

4.1.25. Synthesis of berberrubine (7)

Commercially available berberine (30.00 g) chloride was heated at 190 °C in a vacuum oven under reduced pressure (20 mm Hg) for 15 min to obtain berberrubine **7** (25.51 g) in 88.4% yield in agreement with the literature.[23]

Acknowledgments

This work was partially supported by National Natural Science Foundation of China [Nos. 21172181, 81250110089, 81250110554 (the Research Fund for International Young Scientists from International (Regional) Cooperation and Exchange Program)], the Key Program of Natural Science Foundation of Chongqing (CSTC2012jjB10026), the Specialized Research Fund for the Doctoral Program of Higher Education of China (SRFDP 20110182110007), the Research Funds for the Central Universities (Nos. XDJK2011D007, XDJK2012B026).

Supplementary data

Supplementary data (NMR spectra for all of the synthesized compounds) associated with this article can be found, in the online version, at http://dx.doi.org/10.1016/j.bmc.2013.05.007.

References and notes

1. Peng, X. M.; Cai, G. X.; Zhou, C. H. *Curr. Top. Med. Chem.* **2013**, *13* (in press).
2. Zhou, C. H.; Wang, Y. *Curr. Med. Chem.* **2012**, *19*, 239.
3. Zhang, F. F.; Gan, L. L.; Zhou, C. H. *Bioorg. Med. Chem. Lett.* **2010**, *20*, 1881.
4. Zhang, L.; Peng, X.M.; Damu, G.L.V.; Geng, R.X.; Zhou, C.H. *Med. Res. Rev.* **2013**, http://dx.doi.org/10.1002/med.21290.
5. Peng, X. M.; Damu, G. L. V.; Zhou, C. H. *Curr. Pharm. Des.* **2013**, *19*, 3884.
6. Zhang, H. Z.; Damu, G. L. V.; Cai, G. X.; Zhou, C. H. *Eur. J. Med. Chem.* **2013**, *64*, 329.
7. Sutherland, H. S.; Blaser, A.; Kmentova, I.; Franzblau, S. G.; Wan, B.; Wang, Y.; Ma, Z.; Palmer, B. D.; Denny, W. A.; Thompson, A. M. *J. Med. Chem.* **2010**, *53*, 855.
8. Khalaj, A.; Nakhjiri, M.; Negahbani, A. S.; Samadizadeh, M.; Firoozpour, L.; Rajabalian, S.; Samadi, N.; Faramarzi, M. A.; Adibpour, N.; Shafiee, A.; Foroumadi, A. *Eur. J. Med. Chem.* **2011**, *46*, 65.
9. Li, Y.; Luo, Y.; Hu, Y.; Zhu, D. D.; Zhang, S.; Liu, Z. J.; Gong, H. B.; Zhu, H. L. *Bioorg. Med. Chem.* **2012**, *20*, 4316.
10. Lee, S. H.; Kim, S.; Yun, M. H.; Lee, Y. S.; Cho, S. N.; Oh, T.; Kim, P. *Bioorg. Med. Chem. Lett.* **2011**, *21*, 1515.
11. Hernandez-Nunez, E.; Tlahuext, H.; Moo-Puc, R.; Torres-Gomez, H.; Reyes-Martinez, R.; Cedillo-Rivera, R.; Nava-Zuazo, C.; Navarrete-Vazquez, G. *Eur. J. Med. Chem.* **2009**, *44*, 2975.
12. Liu, K.; Zhu, H. L. *Anticancer Agents Med. Chem.* **2011**, *11*, 687.
13. Hu, Y.; Lu, X.; Chen, K.; Yan, R.; Li, Q. S.; Zhu, H. L. *Bioorg. Med. Chem.* **2012**, *20*, 903.
14. Lau, N. P.; Piscitelli, S. C.; Wilkes, L.; Danziger, L. H. *Clin. Pharmacokinet.* **1992**, *23*, 328.
15. Khabnadideh, S.; Rezaei, Z.; Khalafi, N. A.; Motazedian, M. H.; Eskandari, M. *DARU J. Pharm. Sci.* **2007**, *15*, 17.
16. Trivedi, M. N.; Gabhe, S. Y.; Vachhani, U. D.; Patel, R. B.; Shah, C. P. J. *Chem. Pharm. Res.* **2011**, *3*, 313.
17. Burman, W. J. *Clin. Infect. Dis.* **2010**, *50*, S165.
18. Tukulula, M.; Sharma, R. K.; Meurillon, M.; Mahajan, A.; Naran, K.; Warner, D.; Huang, J. X.; Mekonnen, B.; Chibale, K. *ACS Med. Chem. Lett.* **2013**, *4*, 128.
19. Marriner, G. A.; Nayyar, A.; Uh, E.; Wong, S. Y.; Mukherjee, T.; Via, L. E.; Carroll, M.; Edwards, R. L.; Grubber, T. D.; Choi, I.; Lee, J.; Arora, K.; England, K. D.; Boshoff, H. I. M.; Barry, C. E. *Curr. Top. Med. Chem.* **2011**, *7*, 47.
20. Samosorn, S.; Tanwirat, B.; Muhamad, N.; Casadei, G.; Tomkiewicz, D.; Lewis, K.; Suksamrarn, A.; Prammananan, T.; Gornall, K. C.; Beck, J. L.; Bremner, J. B. *Bioorg. Med. Chem.* **2009**, *17*, 3866.
21. Zhang, S. L.; Damu, G. L. V.; Zhang, L.; Geng, R. X.; Zhou, C. H. *Eur. J. Med. Chem.* **2012**, *55*, 164.
22. Kuo, H. P.; Chuang, T. C.; Yeh, M. H.; Hsu, S. C.; Way, T. D.; Chen, P. Y.; Wang, S. S.; Chang, Y. H.; Kao, M. C.; Liu, J. Y. *J. Agric. Food. Chem.* **2011**, *59*, 8216.
23. Bodiwala, H. S.; Sabde, S.; Mitra, D.; Bhutani, K. K.; Singh, I. P. *Eur. J. Med. Chem.* **2011**, *46*, 1045.
24. Gautam, R.; Jachak, S. M. *Med. Res. Rev.* **2009**, *29*, 767.
25. Bahar, M.; Deng, Y.; Zhu, X.; He, S.; Pandharkar, T.; Drew, M. E.; Navarro-Vázquez, A.; Anklin, C.; Gil, R. R.; Doskotch, R. W.; Werbovetz, K. A.; Kinghorn, A. D. *Bioorg. Med. Chem. Lett.* **2011**, *21*, 2606.
26. Vennerstrom, J. L.; Lovelace, J. K.; Waits, V. B.; Hanson, W. L.; Klayman, D. L. *Antimicrob. Agents Chemother.* **1990**, *34*, 918.
27. Fang, B.; Zhou, C. H.; Rao, X. C. *Eur. J. Med. Chem.* **2010**, *45*, 4388.
28. Güven, Ö. Ö.; Erdogan, T.; Göker, H.; Yıldız, S. *Bioorg. Med. Chem. Lett.* **2007**, *17*, 2233.
29. Karegoudar, P.; Prasad, D. J.; Ashok, M.; Mahalinga, M.; Poojary, B.; Holla, B. S. *Eur. J. Med. Chem.* **2008**, *43*, 808.
30. Agudelo, D.; Bourassa, P.; Bruneau, J.; Berube, G.; Asselin, E.; Tajmir-Riahi, H. A. *PLoS One* **2012**, *8*, e53499.
31. Belatik, A.; Hotchandani, S.; Bariyanga, J.; Tajmir-Riahi, H. A. *Eur. J. Med. Chem.* **2011**, *48*, 114.
32. Mallia, M. B.; Subramanian, S.; Mathur, A.; Sarma, H. D.; Venkatesh, M.; Banerjee, S. *Bioorg. Med. Chem. Lett.* **2008**, *18*, 5233.
33. Grimmett, M. R. In *Comprehensive Heterocyclic Chemistry*; Potts, K. T., Ed.; Pergamon: Oxford, 1984; pp 345–456.
34. Li, Y. X.; Wang, J. L.; Cao, D. L.; Liu, L. L.; Song, L. *Chin. J. Exp. Propellan.* **2011**, *34*, 35 (in Chinese).
35. Zhang, C.; Huang, W. L. *J. China Pharm. Univ.* **2003**, *3*, 7 (in Chinese).
36. Iwasal, K.; Kamigauchi, M.; Ueki, M.; Taniguchi, M. *Eur. J. Med. Chem.* **1996**, *31*, 469.
37. Wang, Y. X.; Kong, W. J.; Li, Y. H.; Tang, S.; Li, Z.; Li, Y. B.; Shan, Y. Q.; Bi, C. W.; Jiang, J. D.; Song, D. Q. *Bioorg. Med. Chem.* **2012**, *20*, 6552.
38. National Committee for Clinical Laboratory Standards Approved standard Document, M27-A2, Reference Method for Broth Dilution Antifungal Susceptibility Testing of Yeasts. National Committee for Clinical Laboratory Standards, Wayne, PA, 2002.
39. Zhang, Y. Y.; Zhou, C. H. *Bioorg. Med. Chem. Lett.* **2011**, *21*, 4349.
40. Suryawanshi, V. D.; Anbhule, P. V.; Gore, A. H.; Patil, S. R.; Kolekar, G. B. *Ind. Eng. Chem. Res.* **2012**, *51*, 95.
41. Lakowicz, J. R. *Principles of Fluorescence Spectroscopy*, 3rd ed.; Springer: New York, 2006. pp. 11–12.
42. Lehrer, S. S. *Biochemistry* **1971**, *10*, 3254.
43. Scatchard, G. *Ann. N.Y. Acad. Sci.* **1949**, *51*, 660.
44. Mote, U. S.; Patil, S. R.; Bhosale, S. H.; Han, S. H.; Kolekar, G. B. *J. Photochem. Photobiol., B* **2011**, *103*, 16.